Geologica Acta, Vol.9, Nos 3-4, September-December 2011, 307-328
DOI: 10.1344/105.000001716
Available online at www.geologica-acta.com

geologica acta

The Pelona-Pico Duarte basalts Formation, Central Hispaniola: an on-land section of Late Cretaceous volcanism related to the Caribbean large igneous province

J. ESCUDER-VIRUETE [1] [*] A. PÉREZ-ESTAÚN [2] M. JOUBERT [3] D. WEIS [4]

[1] Instituto Geológico y Minero de España
C. La Calera 1, 28760 Tres Cantos, Madrid. Spain. E-mail: j.escuder@igme.es

[2] Instituto Ciencias Tierra Jaume Almera-CSIC
Lluís Solé Sabarís s/n. 08028 Barcelona, Spain. E-mail: andres@ija.csic.es

[3] Bureau de Recherches Géologiques et Minières
Av. C. Guillemin. 45060 Orléans. France. E-mail: m.joubert@brgm.fr

[4] Pacific Centre for Isotopic and Geochemical Research. University of British Columbia
6339 Stores Road Vancouver, BC V6T-1Z4. Canada. E-mail: dweis@eos.ubc.ca

* Corresponding author

ABSTRACT

Located in Central Hispaniola, the Pelona-Pico Duarte basalts Formation (Fm.) offers an opportunity to study the Late Cretaceous Caribbean large igneous province magmatism on land. It is composed by a ~2.5km-thick pile of massive and monotonous submarine flows of basalts, locally intruded by synvolcanic dikes and sills of dolerite. The Pelona-Pico Duarte basalts Fm. was emplaced onto Turonian-Lower Campanian island-arc volcanic and sedimentary sequences, and is overlain by Maastrichtian platformal carbonates. Two $^{40}Ar/^{39}Ar$ plateau ages indicate both extrusive and intrusive magmatic activity at least during the 79-68Ma interval (Middle Campanian to Maastrichtian), so the magmas were in part coeval with the late phases of the Caribbean large igneous province. The basalts have a restricted major-and trace-element, and isotopic, compositional variation. For a range of 47.6-50.2wt.% SiO_2, the Pelona-Pico Duarte basalts Fm. has relatively high contents in TiO_2 (1.5-3.6wt.%) and Fe_2O_{3T} (10.7-13.1wt.%). On the basis of MgO contents, samples can be classified into tholeiitic basalts (<8wt.%) and high-Mg basalts (8-12wt.%). Mineral assemblages and major element compositional trends indicate that basalts derived from tholeiitic parental magmas by fractionation of olivine plus spinel, clinopyroxene and orthopyroxene, observed as microphenocrysts, as well as plagioclase and Fe-Ti oxides. In a MORB-normalized multi-element plot, the basalts have light rare earth elements (LREE) enriched ($[La/Nd]_N$=1.5-2.2) and heavy rare earth elements (HREE) depleted ($[Sm/Yb]_N$=2.1-3.7) patterns, with very high Nb contents (11-30ppm). These patterns and the values of trace element ratios (K/Ba<20, Ti/V>20 and Zr/Nb<10) are characteristic of transitional and alkalic oceanic-island basalts. In terms of Sr-Nd isotopic composition, the samples are homogeneous and enriched relative to older Caribbean large igneous province units in Hispaniola, with $(^{87}Sr/^{86}Sr)_i$ ratios between 0.70330

and 0.70348 for a very restricted range of $(\varepsilon_{Nd})_i$ values between +5.0 and +5.9 (where *i*=70Ma). The Pelona-Pico Duarte basalts Fm. are interpreted as partial melts of a plume-related, deep enriched source, which have not been contaminated by active subduction. Mantle melt modelling indicates that both high-Mg basalts and basalts formed by mixed melts of both garnet and spinel lherzolite in variable amounts. Melts incorporated at different mantle depths, most probably in relation to the melt column processes in an upwelling plume.
The Pelona-Pico Duarte basalts Fm. has significantly different values of petrogenetic tracers compared to underlying arc-related lavas, indicating a fundamental change in the mantle sources. It has geochemical affinities with the mantle domain influenced by the Late Cretaceous Caribbean plume, suggesting that enriched mantle was flowing toward the NE, to the mantle wedge region of the Caribbean island-arc, in response to rollback of the SW-directed subduction of the proto-Caribbean slab.

KEYWORDS | **Caribbean large igneous province. Mantle source. Hispaniola. Caribbean plate.**

INTRODUCTION

Most Late Cretaceous lavas in Hispaniola have a typical subduction-related geochemical signature and therefore record the magmatic activity of the Caribbean paleoisland-arc (Lewis et al., 1991; Lebron and Perfit, 1994). Nevertheless, thick sequences of volcanic rocks cropping out in the axial sector of the Cordillera Central have trace element and isotopic compositions with an enriched mid-ocean ridge basalt (E-MORB) to ocean island basalt (OIB) affinities (e.g. Ba/La<40, La/Yb>10, ε_{Nd}=+6 to +8; Escuder-Viruete et al., 2008). These magmas intruded into and extruded onto arc volcanic rocks of the Cenomanian-Lower Campanian Tireo Group and related intrusions of gabbros and tonalites. Therefore, mantle wedge-derived Caribbean island-arc magmatism was replaced by non-arc-like magmatism during the uppermost Late Cretaceous in Central Hispaniola. These relations raise questions about the timing of formation of these non arc-like magmas, the relatively fast change of magma sources, their relationship with the Caribbean large igneous province (in the sense of Sinton et al., 1998; Hauff et al., 2000; Hoernle et al., 2004), and the Late Cretaceous geodynamical evolution of the northeast edge of the Caribbean plate.

A hypothesis is that change in the magmatism was induced by Caribbean arc-rifting, extension and, eventually, back-arc basin development and, as a result, it had an origin from processes not directly related to a Caribbean mantle plume. During arc rifting and back-arc development a changing style in the petrogenesis of the magmas and nature of the mantle sources occurs. And these characteristics evolve from those typical of volcanic arcs to those of sea-floor spreading (Gribble et al., 1998; Ewart et al., 1998; Taylor and Martínez, 2003). Physical models proposed for this evolution imply a reorganization of mantle convective regimes beneath evolving back-arc basins, where an advective system similar to that of mid-ocean ridges is superimposed on a suprasubduction zone corner flow field (Martínez and Taylor, 2002). Owing to continued spreading, the extension axis separates from the volcanic front and the flux of fluids/melts from the subducting slab to the mantle wedge decreases (Walker et al., 2003). Mantle source changes when, eventually, the back-arc spreading system separates sufficiently from the volcanic front and it is not significantly affected by hydration and slab-derived geochemical components (Martínez and Taylor, 2002). In this tectonic context, fertile MORB-source mantle must be advecting into the mantle wedge to balance the overall roll-back of the subducting slab. Such a mantle flow has been inferred under back-arcs on the basis of temporal changes in geochemical and isotopic signature of basin lavas (Taylor and Martínez, 2003), mapping upper mantle seismic anisotropy (Smith et al., 2001), laboratory analogical modelling (Kincaid and Griffiths, 2003), and thermomechanical numerical modelling (Nikolaeva et al., 2008).

In this tectonic context, the change of magma sources recorded in Central Hispaniola during the Late Cretaceous might be the consequence of mantle flow that drags the plume source of the Caribbean large igneous province under the extended island-arc. In this paper, we examine the field relationships, petrography, Ar-Ar geochronology, major trace elements and Sr-Nd isotopic compositions of the Pelona-Pico Duarte basalts Fm. from Central Hispaniola to assess the nature of the mantle source, the conditions of melting and the magmatic history of the region in the context of the construction of the Late Cretaceous Caribbean large igneous province. These data, in conjunction with published data of coeval island-arc and Caribbean plateau-related units in Hispaniola, allow us to address two main issues: 1) the change of mantle sources in the late Cretaceous; and 2) the original tectonic setting of the basalts. Finally, we propose a tectonomagmatic evolutive model for Central Hispaniola during the Campanian-Maastrichtian.

GEOLOGICAL SETTING

The Caribbean large igneous province

The Caribbean large igneous province formed in a period of extreme magmatic activity in the Late Cretaceous which originated an oceanic plateau that was subsequently incorporated in the Caribbean plate (Kerr et al., 1997; Sinton et al., 1998; Hauff et al., 2000; Hoernle et al., 2002). The submerged portion of the plateau in the Caribbean Sea was sampled by drilling during Deep Sea Drilling Project Leg 15 and Ocean Drilling Programme Leg 163 (Donnelly et al., 1990). The on-land portion was sampled in exposed sequences of the Caribbean large igneous province outcrop in Jamaica, Hispaniola, Puerto Rico, coastal borderlands of Venezuela, Curaçao and Aruba islands, the Pacific coast of Central America and western Colombia and Ecuador (Lapierre et al., 2000; Kerr et al., 2002). The Caribbean large igneous province includes volcanic rocks erupted during three phases of broadly different age: 124-112Ma (Lapierre et al., 2000; Escuder-Viruete et al., 2007b), 94-83Ma (the main magma production phase; Kerr et al., 1997; Sinton et al., 1998; Hastie et al., 2008) and 80-72Ma (Révillon et al., 2000). These phases have also been recognized by Hauff et al. (2000) and Hoernle et al. (2004) in Costa Rica and in other Cretaceous oceanic plateaus from the Western Pacific (Kerr, 2003), where plume magmatism occurred for 50Ma or more at variable eruptive rates. The youngest Caribbean large igneous province rocks are found in the Dominican Republic (69Ma) and the Quepos Peninsula of Costa Rica (63Ma; Sinton et al., 1998). Thus, magmatism of the Caribbean large igneous province magmatism occurred from the Aptian to the Maastrichtian, with a peak at around the Turonian-Coniacian (92-88Ma), and not in one voluminous burst at ~90Ma, as was originally postulated.

A Pacific origin for the Caribbean plateau is generally accepted (e.g., Duncan and Hargraves, 1984; Pindell et al., 2005), especially in light of evidence that fragments of oceanic crust were accreted to the margins of the Caribbean region, as in Hispaniola and Puerto Rico, which are closely associated with radiolarian cherts containing fauna of Pacific provenance (Montgomery et al., 1994; Baumgartner et al., 2008; Jolly et al., 2008; Escuder-Viruete et al., 2009). Modelling of the plate tectonic evolution suggests that the eastward movement of the Farallon plate in the Late Cretaceous-Early Tertiary forced the motion of the northern half of the Caribbean large igneous province into the ocean basin that had been opening between North and South America since the Jurassic (Mann, 1999; Pindell et al., 2005). However, the mechanism of motion toward the NE of the plateau remains unclear, especially its relation with the Campanian initiation of subduction in the Costa Rica-Panama arc (see revision of Pindell and Kennan, 2009). Using a fixed hotspot reference frame, Duncan and Hargraves (1984) suggested that the magmas of the Caribbean large igneous province were produced by partial melting within the initial "plume head" of the Galápagos hotspot. However, Meschede (1998) argued against a Galápagos origin for the Caribbean large igneous province and Kerr and Tarney (2005) proposed that the Caribbean large igneous province results from the accretion of two separated Late Cretaceous oceanic plateaus, related to two independent hotspots.

The sequence of melting events associated with a mantle plume (or plumes) that occurred beneath the Caribbean plate is not well established because the internal volcanic stratigraphy of the igneous province is not well known. The uppermost surface of the Caribbean large igneous province has been identified seismically as the B discontinuity, which is interpreted to be the upper surface of the plateau lavas (Mauffret and Leroy, 1997). The discontinuity has been drilled in five localities of the Caribbean basin: Deep Sea Drilling Project sites 146, 150, 151 and 152, and Ocean Drilling Programme Site 1001. At Deep Sea Drilling Project Site 152 and Ocean Drilling Programme Site 1001 (only ~40km far away), a thin basalt sill overlying the basement was drilled, but the basement was not reached. The compositional similarity of basalts from sites 152 and 1001 has led to the suggestion that they are part of the same horizon (Sinton et al., 1998). The basalt sill penetrated at site 152 intrudes Campanian (83-70Ma) sediment, and ^{40}Ar-^{39}Ar dating of basalts from site 1001 yields ages of around 81Ma (Sinton et al., 2000). Basalts are therefore younger than the main phase of plateau construction (i.e. ~90Ma), and also appear to be part of a different seismic horizon (Mauffret et al., 2000). Thus, the basalts sampled at sites 152 and 1001 may not be part of the bulk plateau, but rather the product of late-stage rifting of the Caribbean crust after plateau formation (Sinton et al., 1998). Samples recovered by submersible from the Beata Ridge, a topographic high in the central Caribbean basin, show this structure to be composed mainly of gabbros, dolerites and rare pillow basalts (Révillon et al., 2000), with a geochemical signature very similar to that of basalts from other parts of the Caribbean large igneous province. Most samples have ages between 80 and 75Ma, which are consistent with previous ages within the province, but others are very young, around 55Ma. Following Révillon et al. (2000), the "Galápagos" hotspot was probably responsible for the main plume-related magmatic event at 90Ma, and the 76Ma and 55Ma episodes are related to lithospheric thinning of the Central Caribbean (Mauffret and Leroy, 1997).

Though the Caribbean large igneous province comprises a wide diversity of basaltic magma compositions, the vast majority of the lavas show signatures with ε_{Nd} ranging from

+8.5 to +6 and flat to slightly LREE-enriched chondrite normalized patterns (Kerr et al., 1997, 2002; Sinton et al., 1998; Hauff et al., 2000; Lapierre et al., 2000; Révillon et al., 2000; Thompson et al., 2004; Jolly et al., 2007; Escuder-Viruete et al., 2008). The existence of a very similar geochemical and isotopic signature for basalts of ages from 124 to 63Ma, and from very distant parts of the Caribbean, raises questions about the validity of generally accepted rising mantle-plume models for the formation of the whole Caribbean large igneous province. Therefore, alternative models that reconcile geologic data, petrology and plate tectonic history should be considered.

Occurrences of the Caribbean large igneous province in Hispaniola

In Hispaniola, fragments of obducted/accreted oceanic plateau-like basalts include the Dumisseau Fm. in southwestern Haiti (Sen et al., 1988), equivalent lithostratigraphic units in the Sierra de Bahoruco in southwestern Hispaniola (Escuder-Viruete et al., 2008), the Siete Cabezas Fm. (Donnelly et al., 1990; Sinton et al., 1998), and the Duarte Complex in Central Cordillera (Lewis et al., 1991; Lapierre et al., 1997, 2000; Lewis et al., 2002; Escuder-Viruete et al., 2007b). The Dumisseau Fm. consists of pillow and massive basalt flows and minor picrites interlayered with pelagic limestones, volcanogenic and biogenic turbidites, cherts, and siltstones. Fossil ages of the sediments are Early Cretaceous to Santonian for the lower basalts, and Late Campanian for the upper basalts. Sinton et al. (1998) obtained ^{40}Ar-^{39}Ar ages between 88.7±1.5 and 92.0±4.8Ma for the lower basalts. However, the upper basalts of the Dumisseau Fm. should be younger, given the Late Campanian fossil age of the sediments and the 75.0±1.5Ma K-Ar age provided by a late-stage sill intruding the upper sequence (Sen et al., 1988). This formation is overlain by late Campanian to Maastrichtian limestones. In Central Hispaniola, the Siete Cabezas Fm. unconformably overlies the Duarte Complex directly (Escuder-Viruete et al., 2008). It is composed of massive and pillowed aphyric basalts, with minor pyroclastic breccias, vitric tuffs and cherts, intruded by dolerite dikes. Radiolarian content in the sediments yields a Middle Campanian to Maastrichtian age (Montgomery and Pessagno, 1999). Sinton et al. (1998) obtained consistent ^{40}Ar-^{39}Ar ages by whole-rock (69.0±0.7Ma) and plagioclase (68.5±0.5Ma) analyses. These ages and the geochemical characteristics of the lavas (tholeiitic basalts with flat REE patterns) led Lewis et al. (2002) to attribute this unit to the Caribbean large igneous province. The Duarte Complex comprises a ~3km thick sequence of heterogeneously deformed and metamorphosed mafic to ultramafic volcanic rocks, intruded by Late Cretaceous arc-related batholiths (91-83Ma; Escuder-Viruete et al., 2007a, 2008). The complex includes olivine-clinopyroxene phyric meta-picrites and high-Mg meta-basalts, chemically related to plume-generated magmas (Lewis et al., 2002) and similar to the most enriched Caribbean large igneous province lavas (Lapierre et al., 1997, 2000; Escuder-Viruete et al., 2007b). Foliated amphibolites of the Duarte Complex yield ^{40}Ar-^{39}Ar hornblende plateau ages of 93.9±1.4 and 95.8±1.9Ma (Cenomanian) that demonstrate an older age of the protholiths, probably Albian (>96Ma). Therefore, this complex records an Early Cretaceous phase of the Caribbean large igneous province construction in Hispaniola.

Structural blocks in Central Hispaniola

Central Hispaniola is a composite of oceanic derived units bound by the left-lateral strike-slip Hispaniola fault zone and the San Juan-Restauración fault zone (Fig. 1). Accreted units mainly include the serpentinized Loma Caribe peridotites, MORB-type gabbros and basalts, Late Jurassic deep-marine sediments, Cretaceous volcanic units related to the Caribbean large igneous province, and Late Cretaceous arc-related igneous and sedimentary rocks (Draper and Lewis, 1991; Lewis et al., 1991, 2002; Escuder-Viruete et al., 2007a, 2009; Lapierre et al., 1997, 1999). These units were variably deformed and metamorphosed in prehnite-pumpellyte, greenschist and amphibolite facies conditions, but the textures of the protoliths are often preserved. The internal structure of Central Hispaniola is characterized by several km-scale NNW-SSE to WNW-ESE trending fault zones (Fig. 2), which bound three crustal domains or tectonic blocks, namely: Jicomé, Jarabacoa, and Bonao. These tectonic blocks are characterized by different Turonian-Campanian volcanic stratigraphies, geochemical compositions and physical characteristics of their constituent igneous rocks (Escuder-Viruete et al., 2008). The Loma de Cabrera, Loma del Tambor, Macutico and Arroyo Caña gabbro-tonalitic batholiths were intruded syn- to late-kinematically along these shear and fault zones mainly during the Coniacian-Santonian interval (90-84Ma; Escuder-Viruete et al., 2006). Turbiditic sedimentary basins filled with the Tavera Group, which was unconformably deposited over these juxtaposed tectonic blocks, indicate that the main ductile structure of Central Hispaniola was pre-Middle Eocene. Late Cretaceous fault zones were variably reactivated during the Upper Eocene-Oligocene brittle thrusting and the Miocene to Recent uplift of the Cordillera Central.

The Jicomé block is composed of a >3km thick sequence of arc- and Caribbean large igneous province-related volcanic, subvolcanic and volcano-sedimentary rocks of the Tireo Group and the overlying Peña Blanca and Pelona-Pico Duarte Fms. (Fig. 2). The Tireo Group includes two main volcanic sequences with different geochemical characteristics (Escuder-Viruete et al., 2007a).

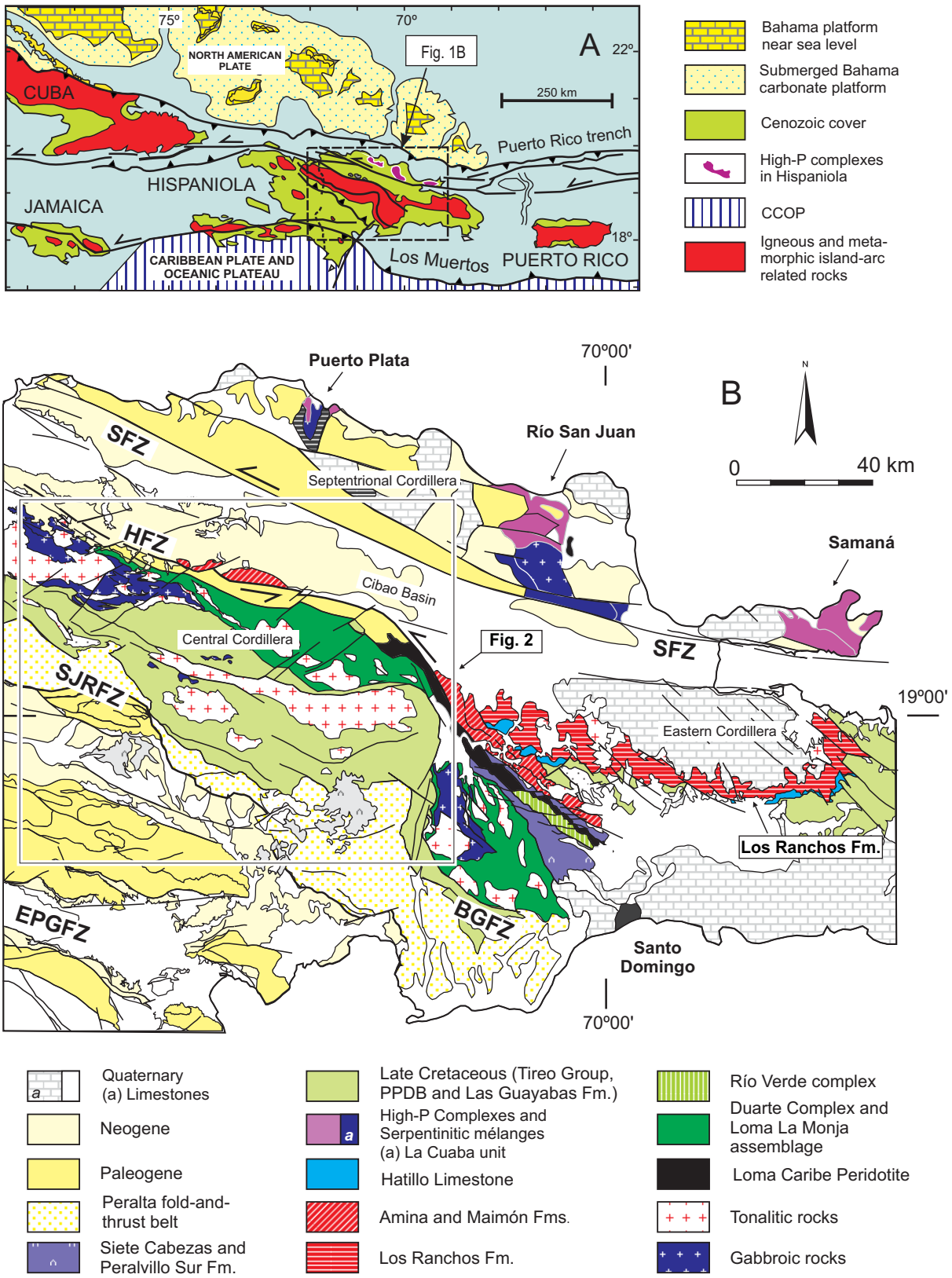

FIGURE 1 | **A) Map of the northeastern Caribbean plate margin. Box shows location of the study area. B) Schematic geological map of Central, Septentrional and Eastern Cordilleras in Hispaniola. SFZ: Septentrional fault zone; HFZ: Hispaniola fault zone; BGFZ: Bonao-La Guácara fault zone; SJRFZ: San José-Restauración fault zone; EPGFZ: Enriquillo-Plantain Garden fault zone. Box shows location of Fig. 2.**

The lower Constanza Fm. constitutes an Albian to Turonian tholeiitic suite, dominated by submarine vitric-lithic tuffs and breccias of basaltic to andesitic composition, with minor interbedded basaltic flows. The upper Restauración Fm. is characterized by a spatial and temporal association of subduction-related adakites, high-Mg andesites and basalts, and Nb-enriched basalts. This stratigraphic interval is mainly represented by

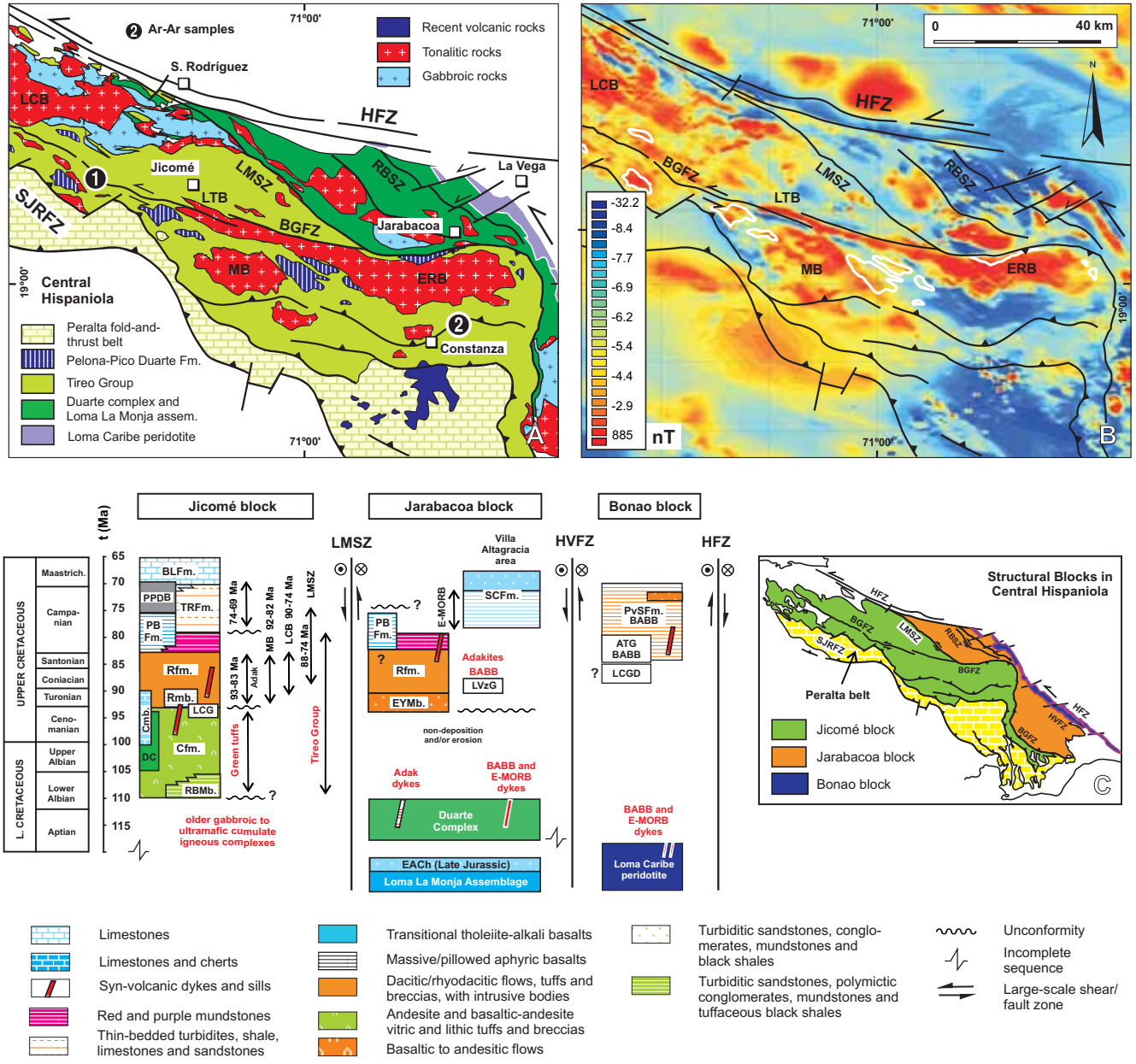

FIGURE 2 | **A) Schematic geological map of the studied area in Central Hispaniola. Encircled numbers show locations of samples for Ar-Ar geochronology. B) Total magnetic field shown. WNW-ESE-trending bands and elongated anomalies correlated respectively with main fault zones and outcrops of gabbro-tonalitic batholiths and basalts of the Pelona-Pico Duarte Fm. (white outlines). C) Schematic lithostratigraphic columns of the three crustal domains or tectonic blocks in Central Hispaniola, namely Jicomé, Jarabacoa and Bonao, as well as of the Eastern Cordillera. LMSZ: La Meseta; RBSZ: Río Baiguaque; HVFZ: Hato Viejo; BGFZ: Bonao-La Guácara shear or fault zones. TG: Tireo Group; RBMb: Río Blanco Member; CFm: Constanza Fm.; DC: Dajabón Chert; CMb: Constanza Member; RFm: Restauración Fm.; LCG: La Cana gabbro; PBFM: Peña Blanca Fm.; BPPD: basalts of Pelona-Pico Duarte Fm.; TRFm: Trois Rivières Fm.; BLFm: Bois de Lawrence Fm.; EYMb: El Yujo Member; LVzG: Los Velazquitos gabbros; SCFm: Siete Cabezas Fm.; ATG: Arroyo Toro gabbros; LCGD: Loma Caribe related-gabbros/diorites; PvSFm: Peralvillo Sur Fm. Ranges of age data in the Jicomé block from Escuder-Viruete et al., (2006a, 2007b, 2008). Adak: adakites; MB: Macutico batholith; LTB: Loma del Tambor batholith; LCB: Loma de Cabrera batholith; LMSZ: La Meseta shear zone; TBA: tholeitic basalt/andesite suite; HMA: high-Mg andesites; NEBA: Nb-enriched basalts and andesites; BABB: back-arc basin basalts. Other abbreviations as in Fig. 1.**

dacitic/rhyolitic explosive volcanism of calc-alkaline affinity, with subaerial to episodic aerial eruptions and emplacement of sub-volcanic domes (Lewis et al., 1991, 2002). Fossil and U-Pb/Ar-Ar geochronological data show that the upper sequence began to extrude at the Turonian-Coniacian boundary (~89Ma) and continued in the Santonian to Lower Campanian. The Peña Blanca Fm. is composed of a 150-250m-thick succession of aphyric, non-vesicular basaltic flows. The basalts have relatively high-Ti contents and high Nb/Th ratios (4-22), as well as slightly LREE-enriched and flat HREE patterns, with a positive Nb anomaly. These characteristics indicate that magmas were derived from a relatively enriched spinel mantle source, which had not been contaminated by a subducting slab (Escuder-Viruete et al., 2008). In the Late Campanian-Maastrichtian, the platform limestones of the Bois de Lawrence Fm. were deposited on top of the extinct arc.

Stratigraphy of the Pelona-Pico Duarte basalts

The Pelona-Pico Duarte basalts Fm. has been defined recently during regional mapping studies (1:50000 scale) of the SYSMIN Project in the Dominican Republic. Exposures of this unit are localized in the axial sector of the Cordillera Central, mainly between 1500 and 3000m of altitude, and are only accessible by walking. However, the strong magnetism of basalts has helped in its cartography. As shown in Fig. 2B, the total magnetic field map of Central Hispaniola is characterized by WNW-ESE trending bands and subparallel elongated anomalies, which are correlated with the main fault zones, and outcrops of the gabbro-tonalitic batholiths and the Pelona-Pico Duarte basalts Fm. (white outlines).

The Pelona-Pico Duarte basalts Fm. is composed of a massive and homogeneous ~2.5km thick pile of basaltic submarine flows, mostly aphyric and amygdalar, frequently banded and rarely porphyritic (Fig. 3). Lava flows are locally interlayered with mafic tuffs, hyaloclastite, and intruded by synvolcanic dikes and sills of basalt and dolerite. Basaltic flows and lobes (<5m thick) are marked mainly by amygdaloidal horizons, often filled by quartz-carbonate in cooling-contraction cracks. Toward the top of the unit, lava flows locally grade to tuff breccias with rare chert clasts. The presence of these breccias on the top of the lava pile suggests that eruptions may have occurred in shallower water; nevertheless, no evidence of subaerial eruptions has been found. Felsic volcanic rocks are absent. In the Loma Guandules area (southeast Restauración), the uppermost flows are overlain by shallow-water limestones of the Bois de Lawrence Fm. (Late Campanian-Maastrichtian). Under the microscope, samples of the Pelona-Pico Duarte basalts Fm. were divided into two main groups: tholeiitic basalts and picritic high-Mg basalts. Tholeiitic basalts typically have a microporphyritic/glomeroporphyritic texture with olivine, Ti-augite, orthopyroxene microphenocrysts in a devitrified glassy to intersertal/subophitic groundmass (Fig. 3). Plagioclase occurs as microprisms in the groundmass and in rarely plagioclase-phyric lavas. High-Mg basalts form massive flow units characterized by a high frequency of euhedral olivine and pyroxene phenocrysts. Accessory phases are small grains of Fe-Ti oxides and apatite. Amygdales and veins are filled by chlorite and quartz, with or without pumpellyte, calcite, zeolite, yellow epidote, albite, clays and opaque minerals.

^{40}AR/^{39}AR-GEOCHRONOLOGY

Analytical results

Two samples were selected for $^{40}Ar/^{39}Ar$ analysis (Fig. 4) with the aim of dating the cooling ages after extrusion of the lavas or emplacement of Pelona-Pico Duarte basalts Fm.-related intrusions. The methodology and the complete data set of the incremental heating ^{40}Ar-^{39}Ar experiments are included in Appendixes I and II. All ages are quoted at the 2σ level of uncertainty. Sample 5873I-SG9015 is a very high-Ti (TiO_2=3.6wt.%) and Nb (25ppm) aphyric basalt from the Loma Guandules in the Restauración area. For seven steps (4-10), the obtained plateau age from whole rock is 68.4±0.75Ma representing 71.0% of the ^{39}Ar released. Sample 6JE13A is a high-Ti (1.6wt.%) and Nb (14.5ppm) basaltic dike, intrusive in the volcanic sequence of the Tireo Group at Constanza. This mafic intrusive has a similar normalized trace element pattern to the one in rocks of the Pelona-Pico Duarte basalts Fm. (see below), indicating that it is probably a feeder dike of the basalts. For seven steps (3-9), the obtained plateau age of hornblende is 79.4±1.0Ma for 86.1% of the ^{39}Ar released.

Interpretation

Fig. 5 includes the Ar-Ar ages obtained for this study and other relevant regional data, which allow us to constrain the duration of the Pelona-Pico Duarte basalts Fm. magmatism and to establish correlations with coeval units of the Caribbean large igneous province. The two $^{40}Ar/^{39}Ar$ whole-rock and hornblende plateau ages obtained from geochemically similar rocks indicate both extrusive and intrusive magmatic activity at least during the 79-68Ma interval (middle Campanian to Maastrichtian; scale of Gradstein et al., 2004). This range of ages for Pelona-Pico Duarte basalts Fm. magmatism is similar to the $^{40}Ar/^{39}Ar$ ages of 69-68Ma obtained for the basalts of the Siete Cabezas Fm. (Sinton et al., 1998) of

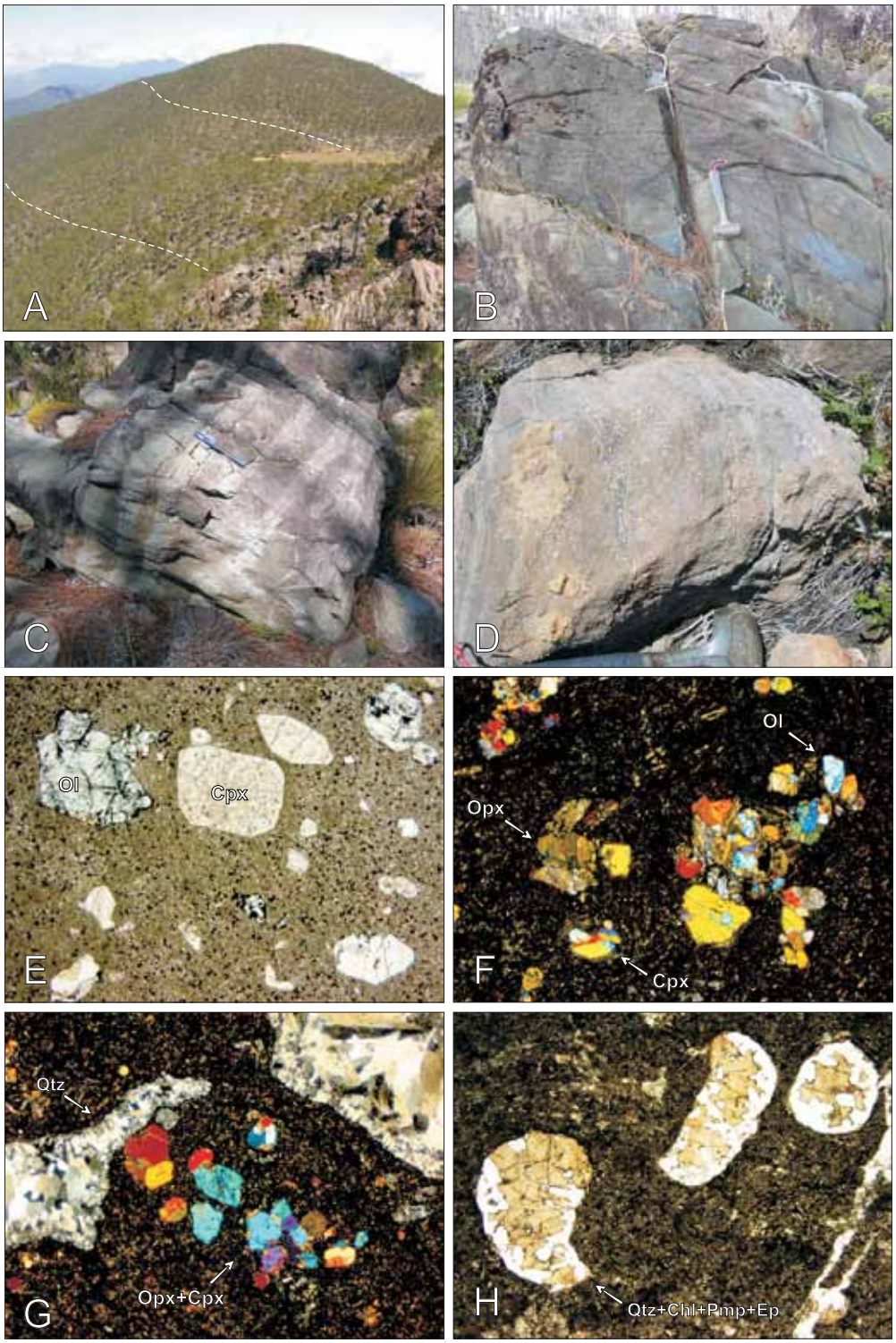

FIGURE 3 | **Field structures: A) Photograph from the Duarte peak (3087m) of ~400m-thick sequence of continuous massive and amygdaloidal flood basalts at the upper stratigraphical levels of the PPDB in the Pelona peak, Central Cordillera, Dominican Republic. The yellow line marks the bedding. B) Massive submarine flows of basalts with margins defined by vesicular and laminated horizons at Lilys valley. C) Massive flows and lobes with amygdaloidal horizons and subparallel infilling of quartz-carbonate in cooling-contraction cracks, south face of El Yaque peak. D) Close-up photograph of stretched vesicules in basaltic flows. Microphotographs: E) Porphyritic basalt with euhedral olivine (Ol; pseudomorphs) and Ti-augite (Cpx) phenocrysts (PPL). F) Basalt with microporphyritic to glomeroporphyritic textures defined by olivine (Ol), clinopyroxene (Cpx) and orthopyroxene (Opx) micro-phenocrysts (XPL). G) Amygdaloidal basalt with micro-phenocrysts of clino and orthopyroxene in a recrystallized glassy to intersertal groundmass rich in Fe-Ti oxides. Note zoned quartz infilling in vesycles (XPL). H) Amygdaloidal and aphyric basalt composed by a recrystallized glassy to intersertal groundmass rich in Fe-Ti oxides and vesycles filled by epidote, quartz and calcite (PPL). Width field in (e) to (h) ~3.5mm.**

the Jarabacoa block, which also have intercalated cherts with radiolarians of middle Campanian to Maastrichtian age (Montgomery and Pessagno, 1999). Also, these ages are similar to those of the Nb-enriched mafic lavas of the Sabana Grande Fm. in southwest Puerto Rico (Campanian; Jolly et al., 2007), the K-Ar age of 75.0±1.5Ma of a sill intruding the upper sequence of the Dumisseau Fm. in Haiti (Sen et al., 1988), and the predominant Campanian magmatic activity recorded in the Beata Ridge (80-75Ma; Révillon et al., 2000); all attributed to the Caribbean large igneous province. Temporarily, this magmatism can be related to the third phase of the Caribbean large igneous province construction (Kerr et al., 2002) and the related volcanic rocks of Costa Rica (Hoernle et al., 2004; Denyer and Baumgartner, 2006; Denyer et al., 2006). In summary, the Ar-Ar ages indicate that the Pelona-Pico Duarte basalts Fm. magmas were in part coeval with the extensive mafic volcanism of the Late Cretaceous Caribbean plateau.

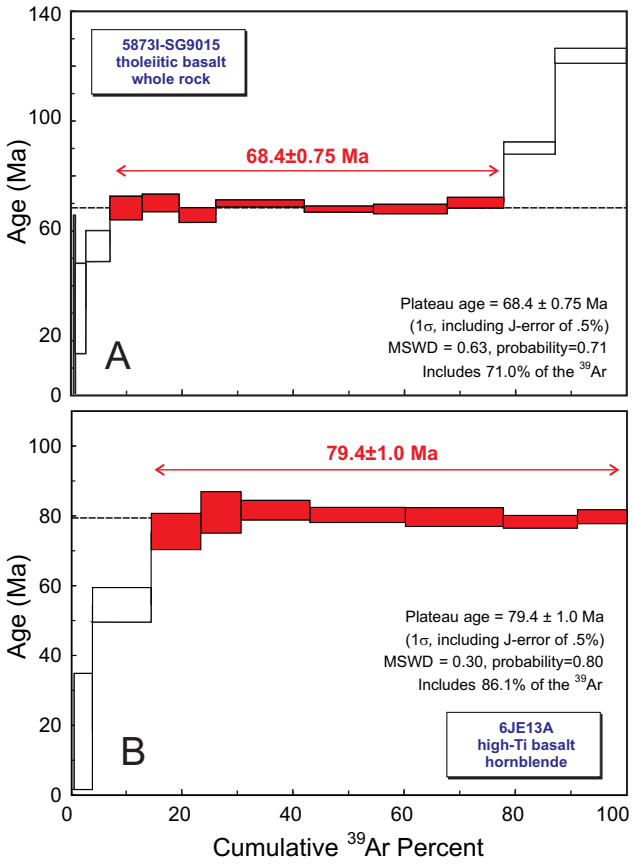

FIGURE 4 | **$^{40}Ar/^{39}Ar$ spectrum of whole rock and hornblende in samples from Pelona-Pico Duarte basalts Fm. and related dikes. The plateau ages were calculated following techniques described in Appendix I. A summary of ^{40}Ar–^{39}Ar incremental heating experiments is in Appendix II. Plateau steps are filled and rejected open. See text for discussion.**

GEOCHEMISTRY

Analytical methods

Samples were powdered in an agate mill, and analysed for major oxides by Inductively-Coupled Plasma-Emission Spectrometry (ICP-ES) and trace elements by Inductively-Coupled Plasma-Mass Spectrometry (ICP-MS). This analytical work was done at the ACME Analytical Laboratories Ltd in Vancouver and the results are reported in Table 1. Details of analytical accuracy and reproducibility are included in Appendix I. A representative subset of samples (Table 2) was also analysed for Sr and Nd isotopic compositions at the Pacific Centre for Isotopic and Geochemical Research of the University of British Columbia. Rb, Sr, Sm and Nd concentrations were measured by a Thermo Finnigan Element2, a double focussing (i.e., high resolution) Inductively Coupled Plasma-Mass Spectrometer (Pretorius et al., 2006). For isotopic analysis, samples were repeatedly leached with HCl6N to remove secondary alteration. Sr and Nd were separated using the method described in Weis et al. (2006). Isotope ratios were measured by a Thermo Finnigan Triton-TI Thermal Ionization Mass Spectrometry (TIMS) in static mode with relay matrix rotation on single Ta filament and double Re-Ta filament for Sr and Nd isotopic analyses respectively. Sr and Nd isotopic compositions were corrected for fractionation using $^{86}Sr/^{88}Sr=0.1194$ and $^{146}Nd/^{144}Nd=0.7219$. During the analyses, the NBS987

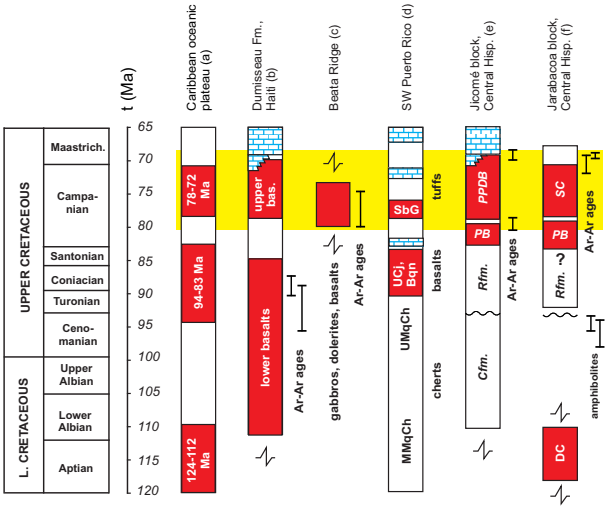

FIGURE 5 | **A) Summary of paleontological and geochronological ages for Caribbean large igneous province units (in black) in the northern Caribbean. Sources; a) Kerr et al. (2002); b) Sen et al. (1988); c) Révillon et al. (2000); d) Jolly et al. (2007); e) this work; and f) Sinton et al. (1998). MMqCh: Middle Mariquita Chert; UMqCh: Upper Mariquita Chert; UCj: Upper Cajul Fm.; Bqn: Boquerón Fm.; SbG: Sabana Grande Fm.; CFm: Constanza Fm.; RFm: Restauración Fm.; PB: Peña Blanca Fm.; PPDB: Pelona-Pico Duarte basalts Fm.; SC: Siete Cabezas Fm. Ar-Ar ages are the error bars (in 2). Time scale from Gradstein et al. (2004).**

TABLE 1 | **Major and trace element data of representative rocks from the Pelona-Pico Duarte Formation and related mafic intrusives**

Map	Manabao							Constanza
X(UTM)	-70.9112	-70.9134	-70.9363	-70.9942	-70.9958	-70.998	-70.951	324221
Y(UTM)	19.0287	19.02553	19.03277	19.03024	19.0273	19.02302	19.03547	2089101
Rock[a]	MBAS	MBAS	MBAS	MBAS	MBAS	MBAS	MBAS	BAS/DOL
Sample	41MJ9020	41MJ9022	41MJ9026	41MJ9033	41MJ9034	41MJ9036	41MJ9044	6JE13A
SiO_2	49.19	48.29	50	43.64	47.6	46.23	49.57	53.31
TiO_2	2.04	2.39	1.35	1.22	1.21	1.35	1.68	1.62
Al_2O_3	14.62	14.29	13.39	13.25	12.74	15.8	13.41	14.19
Fe_2O_3	12.11	13.04	11.6	12.44	11.36	11.84	11.66	11.66
MgO	6.59	6.46	7.19	9.45	9.7	5.45	7.56	5.51
CaO	10.25	9.8	11.78	15.85	12.72	11.95	11.22	4
Na_2O	1.95	1.75	2.16	0.41	1.38	2.31	1.94	4
K_2O	0.25	0.27	0.39	0.11	0.24	1.22	0.28	0.38
P_2O_5	0.174	0.221	0.152	0.131	0.104	0.45	0.139	0.24
MnO	0.18	0.2	0.22	0.22	0.19	0.19	0.21	0.14
Cr_2O_3	0.042	0.034	0.046	0.062	0.08	0.009	0.06	0.006
LOI	2.4	2.9	1.5	2.9	2.4	2.8	2	4.8
C/TOT	0.05	0.03	0.05	0.03	0.08	0.06	0.06	0.07
S/TOT	<0.02	<0.02	<0.02	<0.02	<0.02	<0.02	<0.02	0.08
SUM	99.84	99.67	99.82	99.71	99.80	99.65	99.78	99.86
Mg#[b]	52	50	55	60	63	48	56	48
Cr	-	-	-	-	-	-	-	41.0
Co	41.4	45.5	48.7	63.5	57.2	42	45.9	34.6
Ni	14.7	19.1	47	70.8	81.3	54	42.5	17.0
V	366	414	318	333	320	334	349	253
Rb	4.9	4.2	12	1.3	4	13.4	5.1	3.1
Ba	71	85	119	46	77	387	64	106.5
Th	1.2	1.3	1.3	0.8	1.1	1	1.4	1.3
U	0.4	0.4	0.3	0.3	0.2	0.4	0.4	0.5
Nb	12	15.9	10	8.6	7.9	21.1	9.7	14.5
Ta	0.8	1.1	0.7	0.5	0.6	1.1	0.8	0.9
La	11.6	14.6	10.1	7.1	7.1	16.3	10.1	12.1
Ce	27.9	35.4	22.2	16.1	16.5	31.7	23.7	28.5
Pb	0.6	0.7	0.5	0.3	0.4	0.4	0.3	1.5
Pr	4.05	5.04	3.11	2.35	0.4	4.09	3.33	3.94
Mo	0.2	0.3	1.5	0.7	0.6	0.8	0.7	0.6
Sr	234.7	224.6	222.5	329.3	207.3	313.4	218.6	125.6
Nd	19.4	23.5	14.1	10.8	11.8	16.2	14.6	18.1
Sm	4.72	6.07	3.24	2.99	2.78	3.87	3.88	4.2
Zr	118.2	148.9	88	60.6	59.6	92.9	97.7	113.2
Hf	3.3	4.6	2.5	1.9	2	2.7	2.6	3.2
Eu	1.59	1.83	1.09	1.09	0.94	1.17	1.3	1.42
Gd	5.08	6.31	3.65	3.36	2.99	3.68	4.27	4.2
Tb	0.87	1.07	0.64	0.61	0.51	0.65	0.74	0.8
Dy	4.55	5.92	3.71	3.49	2.91	3.61	3.85	4.05
Y	26.2	32.7	20.9	19.9	16.5	19.6	22.6	21.5
Ho	0.94	1.27	0.78	0.73	0.61	0.73	0.82	0.79
Er	2.49	3.11	2.1	1.84	1.55	1.85	2.12	2.23
Tm	0.37	0.45	0.32	0.31	0.28	0.33	0.34	0.31
Yb	2.2	2.67	1.85	1.69	1.36	1.62	1.85	1.79
Lu	0.33	0.44	0.3	0.28	0.22	0.28	0.31	0.27

Data of samples SG9015, SG9016, SG9017, MJ9377 and MJ9365 are included in Escuder-Viruete et al. (2008).

[a] Rock type abbreviations: DOL, dolerite; MBAS, massive basalt; VBAS, vesicular/amygdalar basalt

Major elements in wt.%; trace elements in ppm.

[b] Mg# = 100 * mol MgO/ mol (FeO + MgO); for $Fe_2O_3/FeO = 0.2$. Total Fe as Fe_2O_3.

TABLE 2 | **Sr-Nd isotope ratios for representative basat samples of Pelona-Pico Duarte Formation**

Sample	Type	Rb	Sr	$^{87}Sr/^{86}Sr$	$(^{87}Sr/^{86}Sr)_i$	Sm	Nd	$^{143}Nd/^{144}Nd$	$(^{143}Nd/^{144}Nd)_i$	$(\varepsilon_{Nd})_i$
6JE68	BAS	4.3	315.4	0.703354 (7)	0.703304	4.08	15.8	0.512923 (7)	0.512831	6.02
MJ9020	BAS	4.9	234.7	0.703540 (8)	0.703480	4.72	19.4	0.512922 (8)	0.512855	5.99
MJ9026	BAS	12	222.5	0.703457 (8)	0.703301	3.24	14.1	0.512896 (7)	0.512833	5.55
MJ9034	HMB	4	207.3	0.703408 (9)	0.703352	2.78	11.8	0.512896 (7)	0.512830	5.51
MJ9036	BAS	13.4	313.4	0.703496 (9)	0.703373	3.87	16.2	0.512890 (8)	0.512824	5.39
MJ9036B	BAS	13.4	313.4	0.703495 (7)	0.703372	3.87	16.2	0.512898 (9)	0.512832	5.54
SG9015	BAS	7.4	346.7	0.703409 (9)	0.703349	7.2	29.9	0.512904 (8)	0.512840	5.64
SG9016	BAS	12	406.7	0.703486 (9)	0.703404	7.5	33.3	0.512869 (7)	0.512809	5.04

All samples were leached and digested on hotplate. BAS; basalts; HMB; high-Mg basalts. Rb, Sr, Sm and Nd values in ppm.
Calculated initial ratios (*i*) and e_{Nd}-values calculated at *t*=70 Ma. Number in brackets is the absolute 2s error in the last decimal places.
e_{Nd} values are relative to $^{143}Nd/^{144}Nd$=0.512638 and $^{147}Sm/^{144}Nd$=0.1966 for present day CHUR (Jacobsen and Wasserburg. 1980) and lambda ^{147}Sm= 6.54×10^{-12}/year

Sr standard gave an average of 0.710253±0.000009 (n=6) and the La Jolla Nd standard gave an average value of 0.511851±0.000013 (n=5). $^{147}Sm/^{144}Nd$ ratio errors are approximately ~1.5%, or ~0.006.

Chemical changes due to alteration and metamorphism

The analyzed basalts have been variably altered and metamorphosed to zeolitic- and prehnite-pumpellyite metamorphic facies conditions. Consequently, changes of the bulk-rock chemistry are expected as a consequence of selected mobility of relevant elements during these processes. Many major (e.g., Si, Na, K, Ca) and trace (e.g., Cs, Rb, Ba, Sr) elements are easily mobilised by late and/or post-magmatic fluids and metamorphism; however, the high field strength elements (HFSE) (Y, Zr, Hf, Ti, Nb and Ta), REE, transition elements (V, Cr, Ni and Sc) and Th, are generally unchanged under a wide range of metamorphic conditions, including seafloor alteration at low to moderate water/rock ratios (Bédard, 1999). Therefore, the geochemical characterization of the Pelona-Pico Duarte basalts Fm. and the petrogenetic discussion will be based mostly on the HFSE and REE, as well as Nd-isotopes, as it can be assumed that they were not significantly affected by alteration or metamorphism.

Major and trace-element compositions

As a suite, the basalts of the Pelona-Pico Duarte basalts Fm. have a very restricted range in SiO_2 content, ranging from 47.6 to 50.2wt.% (Table 1), and high TiO_2 contents between 1.2 and 3.6wt.% (Fig. 6A). On the basis of MgO contents (Fig. 6d), samples can be divided into tholeiitic basalts (<8wt.%) and high-Mg basalts (8-12wt.%). The Mg# values of 63-48 indicate that these lavas have undergone low to moderate amounts of fractionation. They have relatively low contents in CaO (9.8-15.8wt.%) and Al_2O_3 (10.8-14.6wt.%), and relatively high contents in alkalis (2.0-2.6wt.%), P_2O_5 (0.1-0.4wt.%) and Fe_2O_{3T} (11.6-13.0wt.%). These rocks show an increase of SiO_2, Fe_2O_{3T}, TiO_2, CaO, Al_2O_3, alkalis, Zr and Nb, and a decrease in Cr and Ni for decreasing MgO (not all shown in Fig. 6). These trends are tholeiitic and can be attributed to the fractionation of olivine plus Cr-spinel, clinopyroxene and orthopyroxene, observed as microphenocrysts in the lavas, as well as plagioclase and Fe-Ti oxides. These rocks are quartz or olivine normative, with diopside, hyperstene and Cr-spinel. Based on immobile trace element classification schemes (Fig. 7A), the samples are transitional and alkalic basalt (Nb/Y>0.4), which is compatible with their major element compositions, norm and mineralogy. In the tectonic discrimination diagrams of Wood (1980) and Meschede (1986), basalts of the Pelona-Pico Duarte basalts Fm. and related intrusive dikes both plot consistently in within-plate tholeiitic and alkalic basalt fields (Fig. 7B, C).

In a MORB-normalized multi-element plot (Fig. 8), the basalts of the Pelona-Pico Duarte basalts Fm. have LREE enriched ($[La/Nd]_N$=1.5-2.2) and depleted HREE ($[Sm/Yb]_N$=2.1-3.7) patterns, with very high Nb contents (8-30ppm). They do not have positive Pb, K and Sr spikes, and negative Nb-Ta anomalies, typical of subduction-related rocks. However, some samples have a small selective enrichment in some fluid-mobile LILE (Rb, Ba and U), which probably results from seafloor alteration. The slight negative Eu and positive Ti anomalies present in some evolved basalts are related to plagioclase and Fe-Ti oxide fractionation/accumulation, respectively. These patterns and the values of the trace element ratios Ti/V>20 and Zr/Nb<10 (6.2-8.4) are characteristic of modern day transitional and alkalic oceanic-island basalts (Pearce, 2008). The high TiO_2 content and $(Sm/Yb)_N$ ratios suggest that the mantle source of these basalts was relatively enriched and contained garnet (Greene et al., 2009). These rocks are interpreted as partial melts of a plume-related, deep enriched source, which have not been contaminated by active subduction (Nb/Th>8; Fig. 6).

In Fig. 8, the basalts of the Peña Blanca and Siete Cabezas Fm. of the Jicomé and Jarabacoa blocks are plotted for comparison. These sub-alkaline basalts have

distinctive slightly LREE-enriched ($[La/Nd]_N$=1.0-1.8) and flat HREE ($[Sm/Yb]_N$=0.9-1.5) patterns, with a positive Nb anomaly (Nb/Nb*=1.2-2.3). All these features, as well as their incompatible element ratios (Zr/Nb<15 and La/Sm>1.5), are characteristic of enriched MORB (Donnelly et al., 2004). Relatively high-Ti contents, Nb/Th ratios (4-22) and flat-HREE indicate that these magmas were derived from a relatively enriched spinel mantle source, which had not been contaminated by a subducting slab. Probably, these basalts represent a tholeiitic volcanism in distal areas from the arc, such as back-arc areas or dorsal segments affected by mantle plume activity (Escuder-Viruete et al., 2008). On the other hand, the patterns are similar to those of the gabbros and dolerites dredged from the Beata Ridge (Révillon et al.,

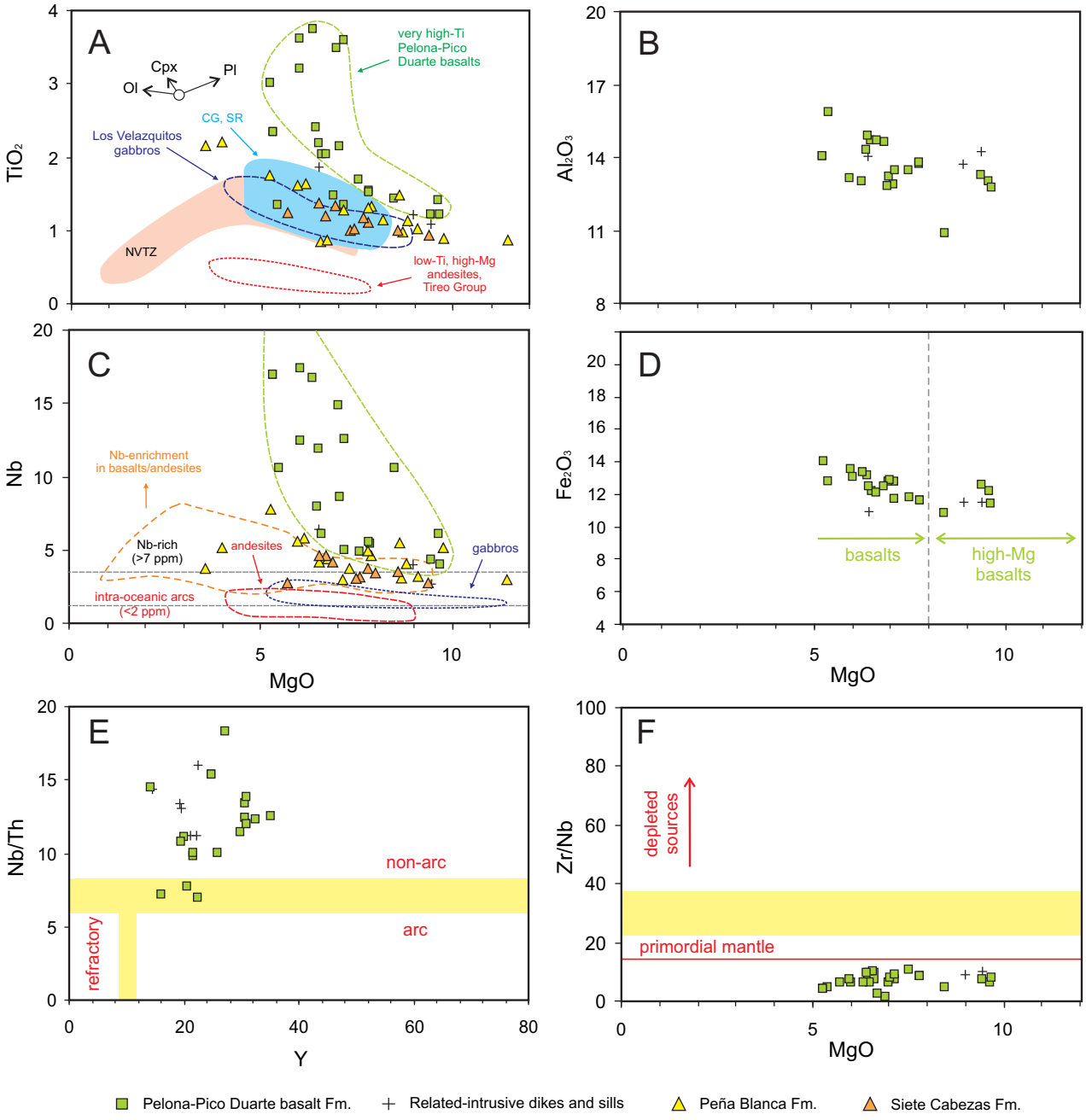

FIGURE 6 | **TiO_2, Al_2O_3, Fe_2O_3, Nb, Zr/Nb *versus* MgO, and Nb/Th *versus* Y, for the basalts, high-Mg basalts and related-intrusive dikes of the PPDB in Central Hispaniola. Basalts from the Peña Blanca and Siete Cabezas Fms. are shown for comparisons. NVTZ, CG and SR fields are Northern Volcano-Tectonic Zone, Central Graben and Spreading ridge fields of the Mariana Arc-Trough system from Gribble et al. (1998), which are shown for comparisons with a modern analogue. Also indicated in (a) are 5% fractional crystallization vectors for olivine (Ol), clinopyroxene (Cpx), and plagioclase (Pl), determined from the average PPDB composition.**

2000), Deep Sea Drilling Project sites 146-153 (except 151; re-analyzed by Jolly et al., 2007) and basalts of the Dumisseau Fm. (Sen et al., 1988). These E-MORB-like characteristics are common in most of the Caribbean large igneous province mafic lavas (Kerr et al., 2002) and suggest a similar Caribbean plume-related source.

Sr-Nd isotopic compositions

The Sr and Nd isotope ratios for basalts and high-Mg basalts of the Pelona-Pico Duarte basalts Fm. are listed in Table 2 and plotted in Fig. 9. The $(\varepsilon_{Nd})_i$ range in all rocks is restricted to values between +5.03 and +6.01 (i=70Ma). $(^{87}Sr/^{86}Sr)_i$ ratio values range between 0.70330 and 0.70348 clustering in the MORB array, which probably reflects that the primary composition has been little modified by subsolidus, hydrothermal alteration. The relatively low $(\varepsilon_{Nd})_i$ values of the Pelona-Pico Duarte basalts Fm. samples are compatible with a relatively homogeneous source dominated by enriched mantle, similar to the enriched MORB mantle composition of Klein (2003), with minimal incorporation of a subducted sedimentary component. This composition is similar to those of other Caribbean large igneous province units (Fig. 9), particularly the most enriched Duarte Complex, Deep Sea Drilling Project Leg 151 and Dumisseau Fm. Therefore, Sr-Nd isotopic compositions of the Pelona-Pico Duarte basalts Fm. suggest that they formed from plume-type mantle containing an enriched component also present in other Caribbean large igneous province units. This similar source also corroborates that the Pelona-Pico Duarte basalts Fm. constitutes an on-land occurrence of the Late Cretaceous Caribbean large igneous province in Central Hispaniola. On the other hand, initial Sr-Nd isotopic ratios values in the basalt of Peña Blanca and Siete Cabezas Fms. basalts define a horizontal trend in Fig. 9 and are restricted to slightly higher $(\varepsilon_{Nd})_i$ values between +6.7 to +7.6, as the relatively depleted Caribbean large igneous province units drilled at the Deep Sea Drilling Project Leg 15. In these basalts, the $(^{87}Sr/^{86}Sr)_i$ ratios are highly variable (0.70302-0.70575), similar to altered rocks in an oceanic environment, and consistent with seawater alteration that shifts the samples from the MORB array to the right (e.g. Hauff et al., 2000a). In summary, during the Late Cretaceous two slightly different Caribbean plume-related sources seem to coexist in Central Hispaniola: the relatively enriched Pelona-Pico Duarte basalts Fm. source and the relatively depleted Peña Blanca and Siete Cabezas Fms. source.

PETROGENESIS AND COMPARISONS

Modelling of mantle melting and magma sources

Introduction to modelling

REE composition of a melt can be particularly diagnostic of source mineralogy and degree of melting; REE are lithophile elements whose behavior has been well characterized and their partition coefficients between major mantle minerals and basaltic melts are well known (Salters and Stracke, 2004). Mantle assemblages containing garnet strongly affect the relationship between light REE (LREE)

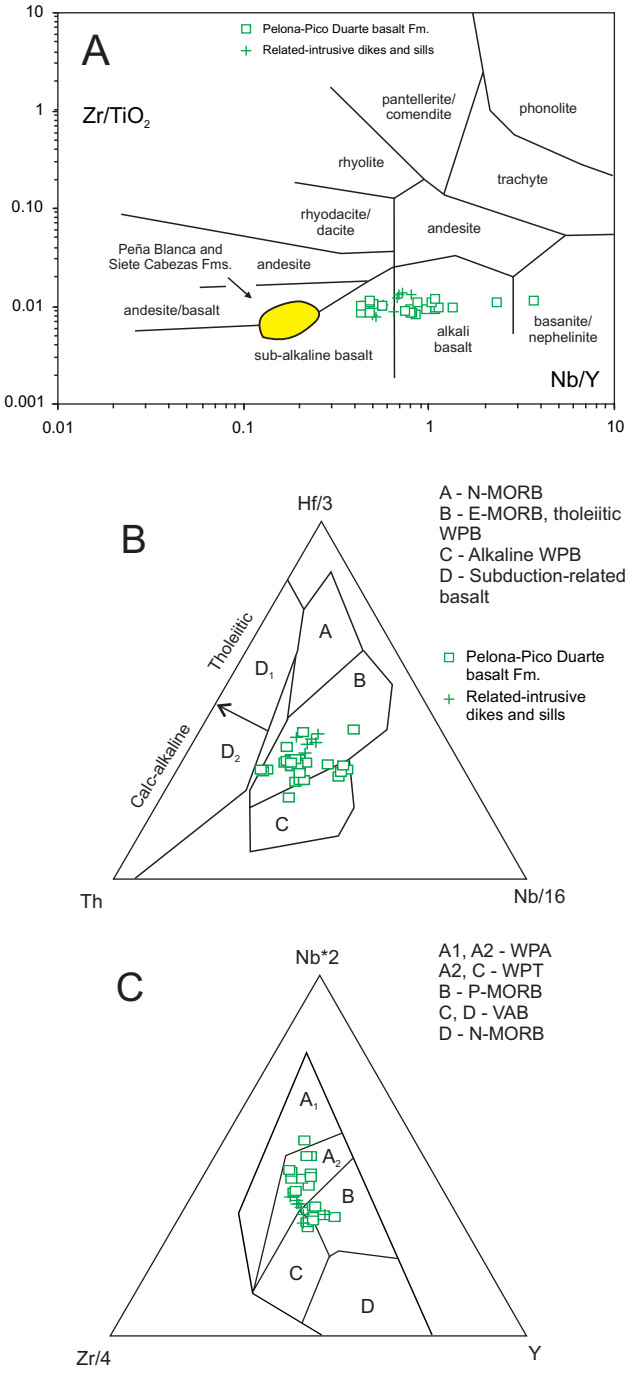

FIGURE 7 | **A) Nb/Y *versus* Zr/TiO$_2$ diagram of Winchester and Floyd (1977), for basalts, high-Mg basalts and related-intrusive dikes of the PPDB in Central Hispaniola, B) Hf-Nb-Th plot with fields defined by Wood (1980), and C) Nb-Zr-Y plot with fields defined by Meschede (1986).**

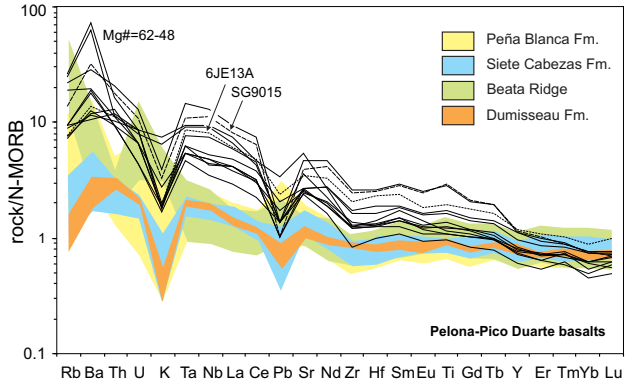

FIGURE 8 | **MORB-normalized multi-element plots for the basalts of the Pelona-Pico Duarte Fm. The fields for geographycally nearest CLIP units are shown for comparison (data taken from Révillon et al., 2000; Sen et al., 1988; Sinton et al., 1998; Escuder-Viruete et al., 2008). Normalization values are taken from Sun and McDonough (1989).**

and heavy REE (HREE) elements, due to the high partition coefficients of the HREE in garnet. For this reason, models of spinel lherzolite and garnet lherzolite melting are used to test the influence of varying source mineralogy on REE concentrations, and on LREE/HREE and MREE/HREE ratios. The approach followed in this study consists of making comparisons between the primitive compositions of the Pelona-Pico Duarte basalts Fm. and the melt calculations for various possible mantle sources.

The details of the model starting assemblages, bulk partition coefficients, and source compositions are summarized in Appendix III. Because the main objective of these calculations is to determine the influence of source mineralogy on the melt composition, the initial chemical compositions have been held constant for both source lithologies and assumed to be the mantle composition of Salters and Stracke (2004). The equation used to derive the melting curves in Figure 10 is the aggregated non-modal fractional melting equation of Shaw (1970):

$$[x_i] = [x_o]\ (1/D_o)\ (1- ((P\ F)/D_o))^{(1/P-1)}$$

where x_i is the concentration in the liquid, x_o is the concentration in the source, D_o is the bulk partition coefficient, F is the degree of melting and P is the proportion in which each phase contributes to the melt.

Source characterization

The results of these calculations suggest that the Pelona-Pico Duarte basalts Fm. melts may have been produced by variable amounts of melting in the garnet and spinel lherzolite fields (Fig. 10). The degree of melting in each field varies slightly depending on the choice of REE ratios used (in this study chrondrite-normalized $[La/Yb]_C$ and $[Tb/Yb]_C$), but garnet lherzolite is always implicated due to the depleted composition in HREE of the lavas of the Pelona-Pico Duarte basalts Fm. Both high-Mg basalts and tholeiitic basalts represent aggregate melts produced from continuous melting throughout the depth of the melting column. In general, all basalts can be produced by mixing of melts in the garnet lherzolite field (generated by 1.6% to 4.0% melting at depth) with melts from the spinel field (produced by melting degrees between 1.8% and 6.0% at low pressure). In Figure 10, the basalts mainly define two groups relative to the melt proportions produced in each field: a) 10-30% garnet lherzolite with 70-90% spinel lherzolite mixing melts, and b) 30-60% garnet lherzolite with 40-70% spinel lherzolite mixing melts. The modelling indicates that the aggregate melts that formed the high-Mg basalts and the less evolved basalts have involved lesser proportions of enriched melts generated at depth, and greater amounts of depleted melts generated at lower pressure (25 garnet lherzolite/75 spinel lherzolite on average). Fraccionated basalts have been produced by higher proportions of melts generated at depth in the garnet stability field (40 garnet lherzolite/60 spinel lherzolite on average). The variable proportion of melts generated and incorporated at different mantle depths are most probably the consequence of melt column processes related to an upwelling plume.

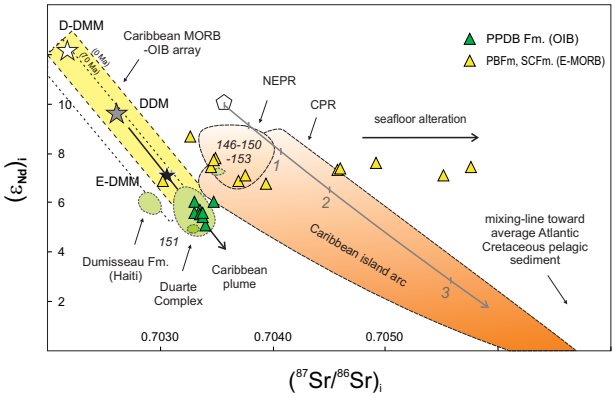

FIGURE 9 | **Initial Sr-Nd isotopes ratios (*i*=70Ma) for the different Late Cretaceous basalts in Central Hispaniola. The fields for the Duarte Complex, DSDP site 15 (CLIP) and Caribbean island-arc lavas from Northeastern and Central Puerto Rico, are taken from Escuder-Viruete et al. (2007a), Hastie et al. (2008; and references therein), Hauff et al. (2000), Jolly et al. (2006, 2007) and Thompson et al. (2004). The MORB-OIB array is defined by the subduction-unmodified lavas from the East Pacific Ridge (data from PETDB, 2007; and references herein). Depleted MORB mantle (DMM) Sr–Nd isotopic compositions are taken from Su and Langmuir (2003): DMM average for MORBs far from plumes; D-DMM is 2σ depleted and E-DMM is 2σ enriched over the average. Field and mantle components are age corrected. Caribbean island-arc field is subparallel to a calculated mixing line between pelagic sediments and representative arc basalt (Jolly et al., 2006; Escuder-Viruete et al., 2008). NEPR: Northeastern Puerto Rico I-III (Albian-Maastrichtian); CPR: Central Puerto Rico I-IV (Albian-Maastrichtian).**

In contrast, the flat HREE compositions of the Peña Blanca and Siete Cabezas Fms. require melting exclusively of a relatively depleted spinel lherzolite source. The results indicate a high degree of melting (8-25%) of this source. Therefore, the mantle source of the Peña Blanca and Siete Cabezas Fms. is shallower and underwent higher degrees of melting than the source of the Pelona-Pico Duarte basalts Fm. However, a small contribution of melts generated in the garnet stability field as small (<1%) non-modal instantaneous fractional melts cannot be ruled out. The basalts from the Deep Sea Drilling Project Leg 15, as well as gabbros and dolerites from the Beata Ridge, are also melts produced by high degrees of partial melting at low pressure of a similar source. However, the basalts from the 151-site proceed from enriched garnet lherzolite sources, as the evolved basalts of the Pelona-Pico Duarte basalts Fm. (Fig. 10).

In summary, melting models suggest the existence of different sources in middle Campanian-Maastrichtian plume-related units of Central Hispaniola: high-Mg basalts and tholeiitic basalts of the Pelona-Pico Duarte basalts Fm. involved deep melting of garnet and spinel lherzolite and were extruded in the Jicomé block; whereas basalts of the Peña Blanca and Siete Cabezas Fms. require high-degree of melting of a more shallower and depleted spinel lherzolite and were extruded in the Jarabacoa block. These sources were unaffected by subduction influence, but basalts were emplaced in Central Hispaniola onto older Cretaceous arc volcanic sequences. Therefore, a change in the source happened through time, which is recorded by changes in the composition of the pre-Middle Campanian mafic igneous rocks.

Changing trace elements and Sr-Nd isotopic compositions through time

A change in the physical characteristics and geochemical compositions of the Late Cretaceous magmatism of Central Hispaniola has been recently proposed by Escuder-Viruete et al. (2008). This change is recorded by distinctive compositional groups of mafic rocks, which correlate with four successive stages in the magmatic evolution (Fig. 11A, B). The >90Ma tholeiitic to calc-alkaline basalts and andesites and associated ultramafic cumulate complexes of stage I represent the older Cenomanian-Turonian Caribbean island-arc magmatism, which is equivalent to coeval magmatism in Cordillera Oriental and Puerto Rico (Jolly et al., 2007, 2008). At 90-88Ma, the onset of extrusion of low-Ti, high-Mg andesites and basalts, Nb-enriched basalts and adakitic dacites to rhyolites characterizes the stage II of arc rift magmatism (Turonian-Coniacian). Immediately following or temporally overlapping the extrusion of felsic volcanics, gabbroic/doleritic and back-arc basin basalt (BABB) -like magmatism intruded and extruded the NE sector of Jarabacoa and Bonao blocks. This BABB-like

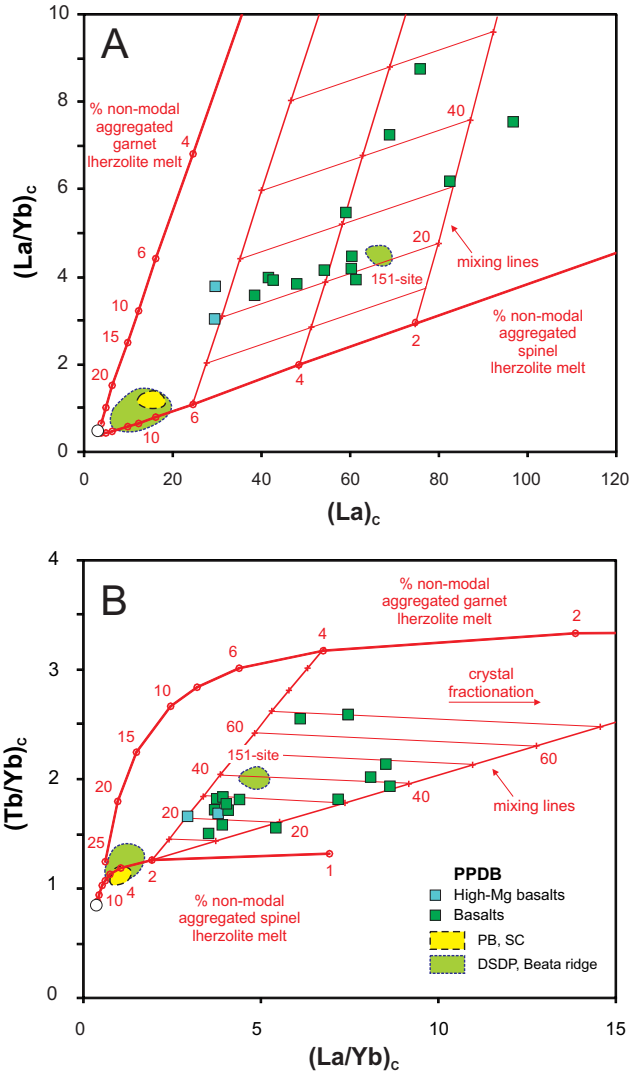

FIGURE 10 | **Results of the non-modal aggregated melt calculations for spinel lherzolite and garnet lherzolite assemblages (solid lines): A) $(La/Yb)_c$ *versus* $(La)_c$ and $(Tb/Yb)_c$ *versus* $(La/Yb)_c$. Gray grid shows mixing between melts produced by variable degrees of spinel lherzolite melt mixed with a 2.5% aggregated non-modal fractional melt of garnet lherzolite. Open square in the lower left hand corner is the depleted mantle composition of Salters and Stracke (2004), used as the source in these calculations. All values on both diagrams are normalized to the chondrite values from Sun and McDonough (1989). Partition coefficients used in the model calculations are from Salters and Stracke (2004), 2.0GPa coefficients were used in the spinel lherzolite melting calculations and the 3.0GPa coefficients were used in the garnet lherzolite melting calculations. The arrow on the right demonstrates the general direction at which crystal fractionation proceeds. Both high-Mg basalts and basalts of the PPDB plot well above the curve generated for spinel lherzolite melting in both diagrams, suggesting that part of the melt generation occurred in the garnet lherzolite field. Basalts from the Peña Blanca and Siete Cabezas Fm., as well as from the DSDP sites 146-150-152-153-site (re-analyzed by Jolly et al., 2008) and the Beata Ridge (Révillon et al., 2000), plot on the lower left side of the diagrams, indicating that melts produced by high degrees of melting in the spinel lherzolite field (i.e. at lower pressure).**

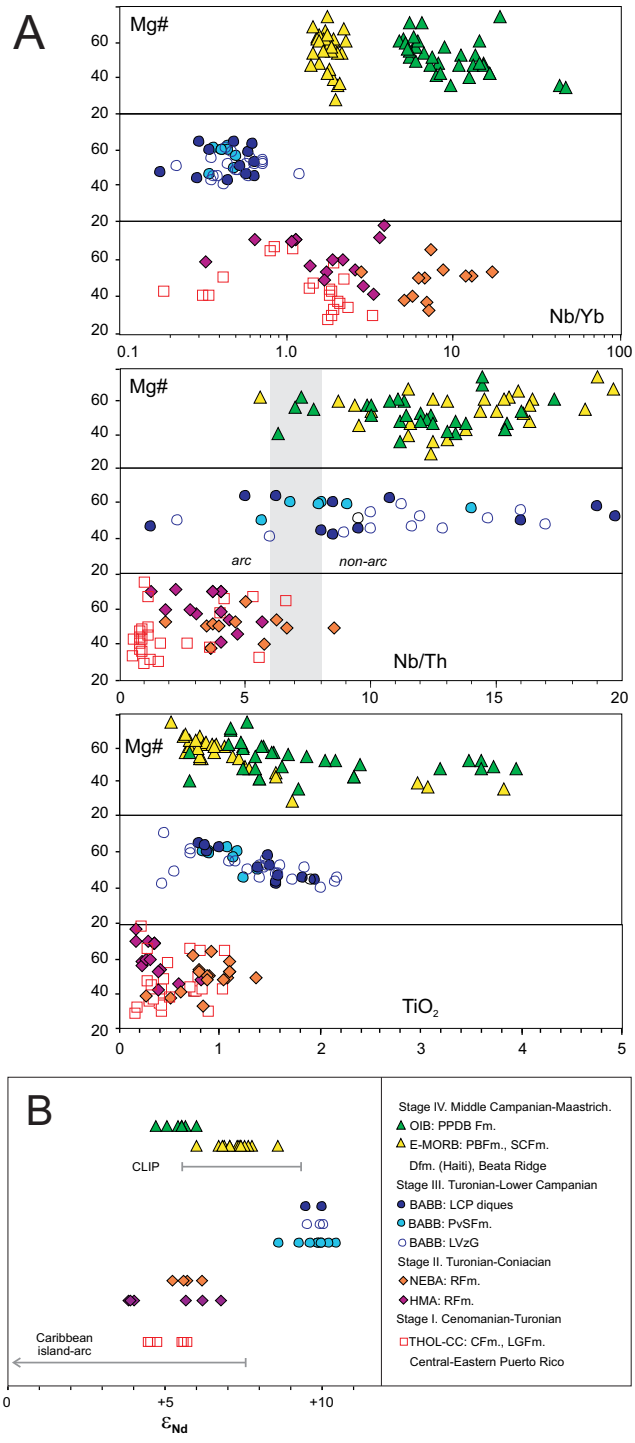

FIGURE 11 | **A) Values of selected geochemical parameters and B) initial ε_{Nd} values for the succesive stages of the Late Cretaceous magmatic evolution of Central Hispaniola (Escuder-Viruete et al., 2007, 2008, this work and unpublished). The Caribbean island-arc volcanic rocks of Puerto Rico are from Jolly et al. (2006, 2007, 2008). Beata Ridge data are from Révillon et al. (2000). THOL: tholeiitic; CC: calc-alkaline; RFm: Restauración Fm.; HMA: high-Mg andesites/basalts; NEBA: Nb-enriched basalts; BABB: back-arc basin basalts; CFm: Constanza Fm.; LGFm: Las Guayabas Fm. (Eastern Cordillera); LCP: Loma Caribe peridotite (Bonao block); LVzG: Los Velazquitos gabbros (Jarabacoa block); PVSFm: Peralvillo Sur Fm. (Bonao block); PBFm: Peña Blanca Fm.; SCFm: Siete Cabezas Fm. (NE sector Jarabacoa block); DFm: Dumisseau Fm. (SW Haiti).**

magmatism, and the related hydrothermal activity and deep-marine sedimentation, represent the Coniacian to Lower Campanian stage III of arc extension. The tholeiitic, transitional and alkalic basalts of the Peña Blanca, Siete Cabezas and Pelona-Pico Duarte Fms. erupted during the Middle Campanian to Maastrichtian and represent the subsequent stage IV of back-arc magmatism. The deposition on top of the platform limestones of the Bois de Lawrence Fm. indicates the ending of magmatic activity in the latest Campanian- Maastrichtian.

This magmatic evolution is shown in Fig. 11 in terms of selected trace elements parameters and isotopic compositions for Late Cretaceous igneous rocks of Central Hispaniola, and suggests changes of the magma sources as a response to geodynamic evolution. Drawn versus Mg# (vol.% MgO/(FeO+MgO) for $Fe_2O_3/FeO=0.2$), or degree of magmatic fractionation, the Ti-content and the Nb/Yb ratio are good parameters to monitorize enrichment and depletion of magma source in low fractionation rocks (Mg#>50), because they should be insensitive to partial melting and largely unaffected by the addition of mobile components from the subducting slab (Pearce and Peate, 1995). By contrast, Nb/Th ratios in arc magma sources are highly susceptible to slab contributions, which enable characterization of arc-like and non-arc-like igneous rocks. In this sense, the low TiO_2 contents (<1wt.%) and low Nb/Th ratio values (<6) of the stage I rocks older than 90Ma in Central Hispaniola (Fig. 11A) suggest derivation from a depleted to very depleted mantle wedge modified by slab-derived components, as is typical for "normal" arc magmatism. However, the magmas related to arc rifting and onset of back-arc spreading, as Mg-rich and BABB-like mafic volcanics of the stages II and III, are mainly characterized by intermediate TiO_2 contents (0.7-2.1wt.%), higher Nb/Th (5-19) and lower Nb/Yb (<7) ratios. These values are typical of a transitional IAT to N-MORB geochemistry and indicate a mantle depleted source progressively less affected by subduction components. The general high TiO_2 contents (0.6-3.9%) and higher Nb/Th (5.5-20) and Nb/Yb (1-14) ratio values of the Peña Blanca, Siete Cabezas and Pelona-Pico Duarte Fm. basalts of stage IV, imply relatively enriched mantle sources and a magmatic activity unaffected by the influence of the subducting slab in the Middle Campanian-Maastrichtian. Therefore, from stages I to IV, the mantle source is progressively more enriched and the subduction component decreased.

Sr-Nd isotope variations permit similar petrogenetic interpretations (Fig. 11b). The Middle-Campanian to Maastrichtian non-arc-like basalts of stage IV have a more restricted range of $(\varepsilon_{Nd})_i$ values (+4.7 to +6.0 for Pelona-Pico Duarte basalts Fm.; +6.8 to +8.6 for Peña Blanca and Siete Cabezas Fm.) than older rocks of the Caribbean island arc stages I and II (generally <+6.8; Escuder-Viruete et al.,

2008), which are extended to lower $(\varepsilon_{Nd})_i$ values as in arc lavas of Eastern Puerto Rico (Jolly et al., 2007, 2008). Also, these restricted $(\varepsilon_{Nd})_i$ values of stage IV are lower than the slightly older mafic rocks of stage III (between +8.6 and +10.5), related to arc rifting. Therefore, the change in the ratio values of Nd-isotopes also records a change in the mantle sources from the slab-influenced island arc-related magmatism of stage I and the arc rifting-related magmas of stage II, to the non-arc-like basalts of stages III and IV. On the other hand, the range of $(\varepsilon_{Nd})_i$ values of the stage IV basalts is similar to those of the mafic rocks sampled in the Beata Ridge, the Deep Sea Drilling Project Leg 15 sites and the Dumisseau Fm of Haití (i.e., the Caribbean large igneous province; Sen et al., 1988; Révillon et al., 2000; Kerr et al., 2002; Jolly et al., 2007; Escuder-Viruete et al., 2008). This suggests that basalts of the coeval Peña Blanca, Siete Cabezas and Pelona-Pico Duarte Fms. are melts that sampled a Caribbean plume component that migrated into the back-arc area of the extended Caribbean island-arc, and this component was relatively more depleted in the basalts extruded in the NE sector of Central Hispaniola.

Tectonomagmatic model

Any model proposed for the tectonic and magmatic evolution of Central Hispaniola during the Late Cretaceous has to explain the following observations: 1) Caribbean island-arc normal magmatism at about ~92-90Ma; 2) in the 90-80Ma interval, a change from mantle-wedge melting affected by slab-derived geochemical components (Restauración Fm.) to mantle melting unaffected by slab-derived components in both Jicomé and Jarabacoa blocks (Peña Blanca Fm.); 3) in the 80-68Ma interval, an extrusion of the non-arc-like basalts of the Siete Cabezas Fm. in the Jarabacoa block (NE sector of Central Hispaniola) and the Pelona-Pico Duarte basalts Fm. in the Jicomé block (SW sector). These basalts are compositionally similar to the depleted and enriched heterogeneous sources of the Caribbean large igneous province.

In orden to explain these observations, we built a model of the Late Cretaceous Caribbean plume magmatism dragged by roll-back of the subducting proto-Caribbean oceanic lithosphere (Fig. 12). The consequences of this slab roll-back for magmatic evolution were: Stage I: the motion towards the SW of the proto-Caribbean subducting slab drives corner flow advection in the mantle wedge. Fluids released by the slab promote partial melting in the mantle, which is progressively depleted of a melt component toward the volcanic front. These melts produced the older than 90Ma tholeiitic to calc-alkaline magmas in the Caribbean island-arc; Stage II: When Caribbean island-arc extension starts, at 90-88Ma, the lithosphere rifts near the rheologically weak volcanic front, and hydrated mantle is advected upward into the stretching and thinning lithosphere, leading to high degrees of melting in the rift phase. As the mantle had been previously depleted, the melts are low-Ti, high-Mg andesites and basalts, extruded in the Jarabacoa block; Stage III: With increasing extension and rifting, an incipient seafloor spreading centre is established near the volcanic front advecting highly hydrated mantle and, as a consequence, BABB-like magmas intruded in the Jarabacoa and incipient Bonao blocks; Stage IV: With continued spreading the extension axis separates from the volcanic front and mantle hydration from the slab decreases. Eventually, at 85-80Ma (Santonian-Lower Campanian) the back-arc spreading system (Bonao block) separates sufficiently from the volcanic front and is not significantly affected by slab-derived geochemical components at this stage. The spreading centre produces MORB-like melts, whose source is modified by a Caribbean-plume enriched component incorporated by lateral flow below the arc from the SW. This plume-related magmatism causes the extrusion of the basalts of Peña Blanca Fm. in the Jarabacoa and Jicomé blocks, and those of the Siete Cabezas Fm. in the Jarabacoa block during the Campanian. At 80-68Ma (Campanian-Maastrichtian), melts derived from a similar but deeper and more enriched Caribbean-plume source gave rise to the off-ridge magmatism of the Pelona-Pico Duarte basalts Fm. in the back-arc area of the Jicomé block.

We speculate if collision of a ridge or other buoyant feature with the subduction-zone forearc at ~90Ma and/or collision of the Cuban forearc with the SE edge of the Maya Block/Caribeana in the Campanian (Pindell et al., 2005; Escuder-Viruete et al., 2007a; García-Casco et al., 2008; Lázaro et al., 2008) might have induced the Caribbean island-arc rifting and subsequent opening of a back-arc basin. Probably, the collision was oblique and diachronic (i.e. older toward the NW) and caused the blockage of the subduction zone in the western segment, where intraoceanic arc accretion and ophiolite emplacement are recorded (García Casco et al., 2008; Talavera-Mendoza et al., 2008; Brueckner et al., 2009). Moreover, collision may also have caused a quick rotation of the Caribbean plate and triggered the migration of the eastern segment of the subduction zone toward the NE, because the Caribbean island-arc remains active in Cordillera Oriental of Hispaniola and Central-Eastern Puerto Rico (Jolly et al., 2007, 2008). In this tectonic scenario, arc roll-back forces induced back-arc opening in Central Hispaniola and dragged the Late Cretaceous Caribbean plume magmatism, similarly to the plate-scale mechanism of collision and induced rotation proposed by Wallace et al. (2005). The structural juxtaposition of the different tectonic blocks that made up Central Hispaniola took place during the closure of the back-arc basin, probably in the Middle Eocene arc-continent hard collision. This is consistent with the Caribbean island-arc burial beneath the unconformable Eocene–Oligocene overlapping sequence of the Tavera Group and with the evolution of the Late

Eocene–Early Miocene syn-collisional turbiditic El Mamey Group farther to the northeast.

Hoerne et al. (2004) establish that the Caribbean large igneous province does not represent a single oceanic plateau, but instead consists of remnants of multiple smaller igneous structures (e.g., oceanic plateaus, paleo-hotspot tracks and flood basalt units) formed over at least 42Ma (125-83Ma). In this sense, the young non-arc-like volcanic rocks at Central Hispaniola and possibly at other locations

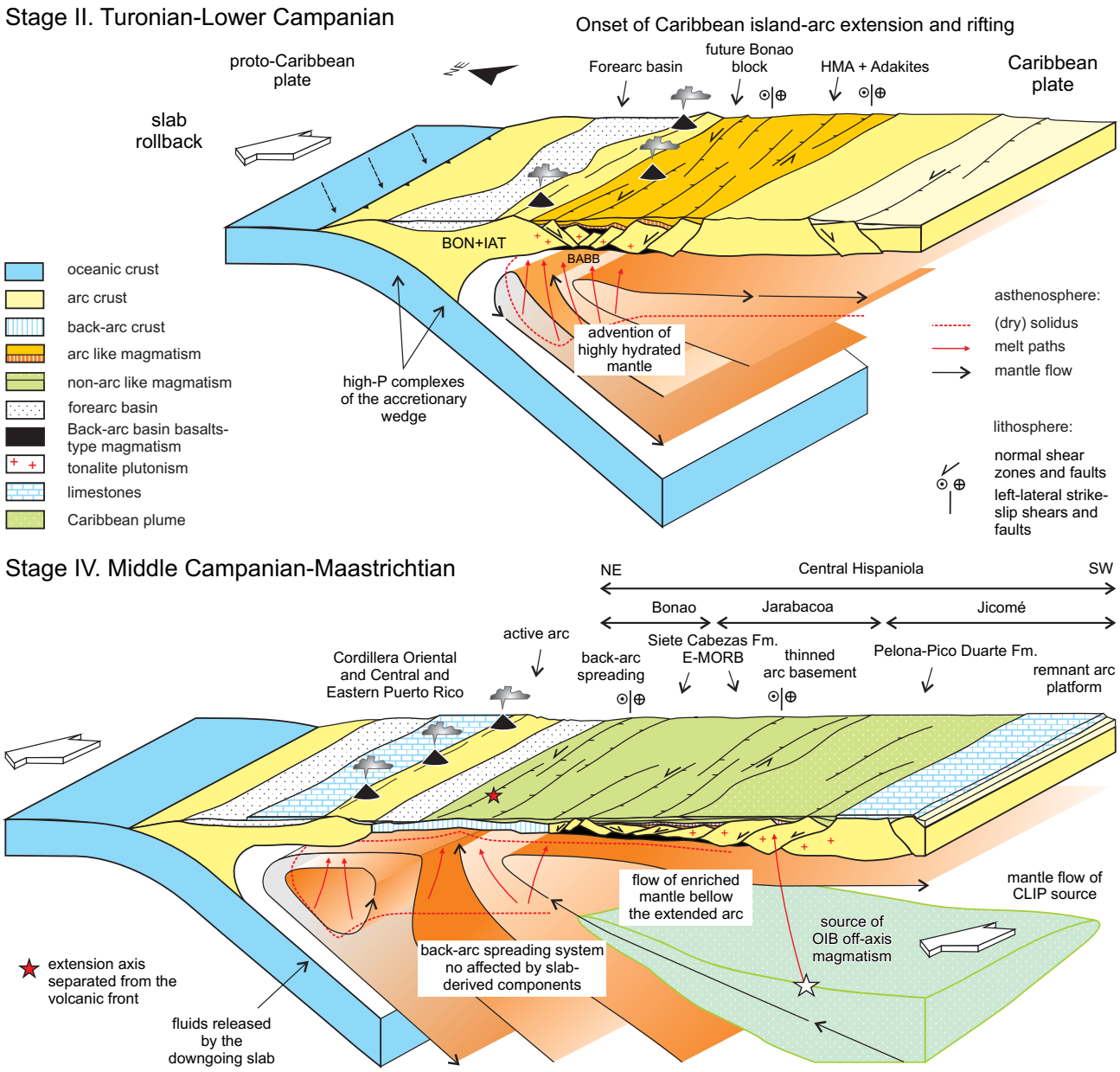

FIGURE 12 | **Schematic tectonomagmatic model for Late Cretaceous magmatic evolution in Central Hispaniola. HMA: high-Mg andesites; NEBA: Nb-enriched basalts; CLIP: Caribbean large igneous province. A) In the Turonian-Coniacian, the SW-directed motion of the subducting proto-Caribbean slab drives corner flow advection in the mantle wedge. Water released by the downgoing slab promotes partial melting in the mantle above the solidus (heavy dashed lines), and generated arc magmatism. When arc extension started, lithosphere rifts near the rheologically weak volcanic front. B) Hydrated mantle is advected upward into the stretching and thinning lithosphere, leading to high degrees of melting in the rift phase and extrusion of high-Mg andesites, and promotes the lower arc crust melting and development of felsic volcanism and tonalitic plutonism. With increasing extension a seafloor spreading centre is established near the volcanic front advecting highly hydrated mantle. As consequence, BABB-like magmas result in a SW position with respect to the volcanic front. In the middle Campanian-Maastrichtian, melts derived from a deeper Caribbean-plume enriched source are incorporated by lateral flow from the SW and produced the OIB-like off-ridge magmatism of the PPDB, which is not affected by slab-derived geochemical components.**

along the northern margin of the Caribbean plate may have been generated through a late-stage pulsing of the plume (78-69Ma), separated from the Pacific mantle by the Costa Rica-Panama subduction zone. Alternatively, they were generated through unrelated and spatially distinct mantle-melting events that sampled similar source material, but they were controlled by plate-scale mechanisms as the previously described.

CONCLUSIONS

The Pelona-Pico Duarte basalts Fm. is composed by a ~2.5km-thick pile of massive and homogeneous flows of basalts, locally intruded by synvolcanic dikes and sills. This volcanic sequence was extruded in a submarine environment at high effusive rate indicated by the absence of intercalated pelagic sediments. Evidences of a subaerial eruptive environment are lacking. The basalts have restricted major- and trace-element and isotopic compositional variations. Mineral assemblages and major element compositions indicate that basalts were derived by fractional crystallization from tholeiitic parental magmas. The samples generally have increasing REE contents at decreasing Mg#, which is a likely effect of fractional crystallization. The relative depletion of HREE in the basalts can be interpreted in terms of partial melting in the stability field of garnet. Sr-Nd isotopic compositions of the Pelona-Pico Duarte basalts Fm. samples plot in the enriched part of the Caribbean MORB-OIB mantle array, as other relatively enriched Caribbean large igneous province units. The relatively low $(\varepsilon_{Nd})_i$ values in the basalts are consistent with the role of an enriched Caribbean plume component in their genesis. Mantle melt modelling suggests that high-Mg basalts and basalts formed by aggregate melts of both garnet and spinel lherzolite sources.The obtained $^{40}Ar/^{39}Ar$ plateau ages of 79-68Ma give evidence that the Pelona-Pico Duarte basalts Fm. volcanism was in part coeval with the Late Cretaceous magmatism of the Caribbean large igneous province, particularly with the 80-75Ma younger event.

The trace element and Sr-Nd isotopic compositions of the Late Cretaceous mafic igneous rocks in Central Hispaniola record an evolution from arc-like to non-arc like magmatism, and suggest a change of the mantle sources through time. These changes are interpreted as the record of proto-Caribbean slab roll-back and migration of the Caribbean island arc volcanic front toward the NE. To balance the roll-back, mantle influenced by the Caribbean plume was advected into the mantle wedge of the extended island-arc. The upwelling of this enriched mantle toward the back-arc spreading centre produced relatively enriched-MORB-type magmas in the Jarabacoa block (NE sector of Central Hispaniola), and off-axis OIB-type magmas in the Jicomé block (SW sector).

ACKNOWLEDGMENTS

The authors thank John Lewis, Gren Draper, Peter Baumgartner and many colleagues of the IGME-BRGM team for help and discussions on the igneous rocks in the Dominican Republic. The Dirección General de Minería of the Dominican Government is also thanked for its support. Elisa Dietrich-Sainsaulieu and Thomas Ulrich are thanked for their help with the Sr-Nd and Ar-Ar isotopic analyses at PCIGR, respectively. This work is part of the MCYT/MCI projects CGL2005-02162/BTE and CGL2009-08674/BTE and also received aid from the cartographic project of the Dominican Republic funded by the SYSMIN Program of the European Union. Careful reviews from Drs. Claudio Marchesi and Domingo Gimeno are much appreciated.

REFERENCES

Baumgartner, P.O., Flores, K., Bandini, A.N., Girault, F., Cruz, D., 2008. Late Triassic to Cretaceous Radiolaria from Nicaragua and Northern Costa Rica–The Mesquito Oceanic terrane. Ofioliti, 33, 1-19.

Bédard, J.H., 1999. Petrogenesis of Boninites from the Betts Cove Ophiolite, Newfoundland, Canada: Identification of Subducted Source Components. Journal of Petrology, 40, 1853-1889.

Brueckner, H.K., Avé Lallemant, H.G., Sisson, V.B., Harlow, G., Hemming, S.R., Martens, U., Tsujimori, T., Sorensen, S.S., 2009. Metamorphic reworking of a high pressure–low temperature mélange along the Motagua fault, Guatemala: A record of Neocomian and Maastrichtian transpressional tectonics. Earth and Planetary Science Letters, 284, 228-235.

Denyer, P., Baumgartner, P.O., 2006. Emplacement of Jurassic-Lower Cretaceous radiolarites of the Nicoya Complex (Costa Rica). Geologica Acta, 4(1-2), 203-218.

Denyer, P., Baumgartner, P.O., Gazel, E., 2006. Characterization and tectonic implications of Mesozoic-Cenozoic oceanic assemblages of Costa Rica and Western Panama. Geologica Acta, 4(1-2), 219-235.

Donnelly, T.W., Beets, D., Carr, M.J., Jackson, T., Klaver, G., Lewis, J., Maury, R., Schellenkens, H., Smith, A.L., Wadge, G., Westercamp, D., 1990. History and tectonic setting of Caribbean magmatism. In: Dengo, G., Case, J. (eds.). The Caribbean Region. The Geology of North America. Geological Society of America, H, 339-374.

Donnelly, K., Goldstein, S., Langmuir, C., Spiegelman, M., 2004. Origin of enriched ocean ridge basalts and implications for mantle dynamics. Earth Planetary Science Letters, 226, 347-366.

Draper, G., Lewis, J.F, 1991. Metamorphic belts in Central Hispaniola. In: Mann, P., Draper, G., Lewis, J.F. (eds.). Geologic and Tectonic Development of the North America-Caribbean Plate Boundary in Española. Geological Society of America Special Paper, 262, 29-46.

Duncan, R.A., Hargraves, R.B., 1984. Plate tectonic evolution of the Caribbean region in the mantle reference frame. In: Bonini, W.E., Hargraves, R.B., Shagam, R. (eds.). The Caribbean-South American plate boundary and regional tectonics. Geological Society of America, 162 (Memoir), 81-93.

Escuder-Viruete, J., 2008. Petrología y Geoquímica de Rocas Ígneas y Metamórficas: Hojas de Polo, La Ciénaga, Enriquillo, Sabana Buey y Nizao. Informe Complementario al Mapa Geológico de la República Dominicana a escala 1:50.000. Santo Domingo, Instituto Geológico y Minero de España-Bureau de Recherches Géologiques et Minières, 57pp.

Escuder-Viruete, J., Contreras, F., Stein, G., Urien, P., Joubert, M., Ullrich, T.D., Mortensen, J., Pérez-Estaún, A., 2006. Transpression and strike-slip partitioning in the Caribbean island arc: fabric development, kinematics and Ar-Ar ages of syntectonic emplacement of the Loma de Cabrera batholith, Dominican Republic. Journal of Structural Geology, 28, 1496-1519.

Escuder-Viruete, J., Contreras, F., Stein, G., Urien, P., Joubert, M., Pérez-Estaún, A., Friedman, R., Ullrich, T.D., 2007a. Magmatic relationships and ages between adakites, magnesian andesites and Nb-enriched basalt-andesites from Hispaniola: record of a major change in the Caribbean island arc magma sources. Lithos, 99, 151-177. doi: 10.1016/j.lithos.2007.01.008.

Escuder-Viruete, J., Pérez-Estaún, A., Contreras, F., Joubert, M., Weis, D., Ullrich, T.D., Spadea, P., 2007b. Plume mantle source heterogeneity through time: insights from the Duarte Complex, Central Hispaniola. Journal of Geophysical Research, 112, B04203. doi: 10.1029/2006JB004323.

Escuder-Viruete, J., Joubert, M., Urien, P., Friedman, R., Weis, D., Ullrich, T., Pérez-Estaún, A., 2008. Caribbean island-arc rifting and back-arc basin development in the Late Cretaceous: geochemical, isotopic and geochronological evidence from Central Hispaniola. Lithos, 104, 378-404. doi:10.1016/j.lithos.2008.01.003.

Escuder-Viruete, J., Pérez-Estaún, A., Weis, D., 2009. Geochemical constraints on the origin of the late Jurassic proto-Caribbean oceanic crust in Hispaniola. International Journal of Earth Sciences, 98, 407-425. doi: 10.1007/s00531-007-0253-4.

Ewart, A., Collerson K.D., Regelous M., Wendt, J.I., Niu, Y., 1998. Geochemical evolution within the Tonga-Kermadec-Lau Arc-Back-arc system: the role of varying mantle wedge composition in space and time. Journal of Petrology, 39, 331-368.

García-Casco, A., Iturralde-Vinent, M.A., Pindell, J., 2008. Latest Cretaceous collision/accretion between the Caribbean Plate and Caribeana: origin of metamorphic terranes in the Greater Antilles. International Geology Review, 50, 781-809.

Gradstein, F.M., Ogg, J.G., Smith, A.G., 2004. A geologic time scale 2004. Cambridge (United Kingdom). Cambridge University Press, 610pp.

Greene, A.R., Scoates, J.S., Weis, D., Nixon, G.T., Kieffer, B., 2009. Melting history and magmatic evolution of basalts and picrites from the accreted Wrangellia oceanic plateau on Vancouver Island, Canada. Journal of Petrology, 50, 467-505.

Gribble, R.F., Stern, R.J., Newman, S., Bloomer, S.H., O'Hearn, T., 1998. Chemical and isotopic composition of lavas from the northern Mariana Trough: implications for magma genesis in back-arc basins. Journal of Petrology, 39, 125-154.

Hastie, A.R., Kerr, A.C., Mitchell, S.F., Millar, I.L., 2008. Geochemistry and petrogenesis of Cretaceous oceanic plateau lavas in eastern Jamaica. Lithos, 101, 323-343.

Hauff, F., Hoernle, K., Tilton, G., Graham, DW., Kerr, A.C., 2000a. Large volume recycling of oceanic lithosphere over short time scales: geochemical constraints from the Caribbean large igneous province. Earth Planetary Science Letters, 174, 247-263.

Hauff, F., Hoernle, K., van den Bogaard, P., Alvarado, G.E., Garbe-Schönberg, D. 2000b. Age and geochemistry of basaltic complexes in western Costa Rica: Contributions to the geotectonic evolution of Central America. Geochemistry, Geophysics, Geosystems, 1(5), 1009, 41pp. doi:10.1029/1999GC000020.

Hoernle, K., Bogaard, P. van den, Werner, R., Lissinna, B., Hauff, F., Alvarado, G.E., Garbe-Schönberg, D., 2002. Missing history (16-71 Ma) of the Galapagos hotspot: Implications for the tectonic and biological evolution of the Americas. Geological Society American Bulletin, 30(9), 795-798.

Hoernle, K., Hauff, F., Bogaard, P. van den, 2004. A 70 Myr history (139-69 Ma) for the Caribbean large igneous province. Geology, 32, 697-700. doi:10.1130/G20574.1.

Jolly, W.T., Lidiak, E.G., Dickin, A.P., 2006, Cretaceous to mid-Eocene pelagic sediment budget in Puerto Rico and the Virgin Islands (northeast Antilles Island Arc). Geologica Acta, 4 (1-2), 35-62.

Jolly, W.T., Schellekens, J.H., Dickin, A.P., 2007. High-Mg andesites and related lavas from southwestern Puerto Rico (Greater Antilles Island Arc): petrogenetic links with emplacement of the Caribbean mantle plume. Lithos, 98, 1-26.

Jolly, W.T., Lidiak, E.G., Dickin, A.P., 2008. Bimodal volcanism in northeast Puerto Rico and the Virgin Islands (Greater Antilles Island Arc): Genetic links with Cretaceous subduction of the mid-Atlantic ridge Caribbean spur. Lithos, 103, 393-414.

Kerr, A.C., 2003. Oceanic Plateaus. In: Rudnick, R. (ed.). The Crust. Oxford, Elsevier Science, Treatise on Geochemistry, 3, 537-565. Avaiable online: www.TreatiseOnGeochemistry.com

Kerr, A.C., Tarney, J., Marriner, G.F., Nivia, A., Saunders, A.D., 1997. The Caribbean–Colombian Cretaceous igneous province: The internal anatomy of an oceanic plateau. In: Mahoney, J., Coffin, M.F. (eds.). Large igneous Provinces. Washington DC., American Geophysical Union (AGU), 123-144.

Kerr, A.C., Tarney, J., Kempton, P.D., Spadea, P., Nivia, A., Marriner, G.F., Duncan, R.A., 2002. Pervasive mantle plume head heterogeneity: evidence from the late Cretaceous Caribbean–Colombian oceanic plateau. Journal

of Geophysical Research, 107, 2140, 13 pp. doi: 10.1029/2001JB0007Kerr, A.C., Tarney, J., 2005. Tectonic evolution of the Caribbean and northwestern South America: The case for accretion of two Late Cretaceous oceanic plateaus. Geology, 33, 269-272. doi: 10.1130/G21109.1.

Kincaid, C., Griffiths, R.W., 2003. Laboratory models of the thermal evolution of the mantle during rollback subduction. Nature, 425, 58-62.

Klein, E.M., 2003. Geochemistry of the Igneous Oceanic Crust. In: Holland, H.D., Turekian, K.K. (eds.). Treatise on Geochemistry. Oxford, Pergamon, 433-463pp. doi: 10.1016/B0-08-043751-6/03030-9.

Lapierre, H., Dupui, V., Lepinay, B.M., Tardy, M., Ruiz, J., Maury, R.C., Hernandez, J., Loubert, M., 1997. Is the Lower Duarte Complex (Hispaniola) a remnant of the Caribbean plume generated oceanic plateau? Journal of Geology, 105, 111-120.

Lapierre, H., Dupuis, V., de Lepinay, B.M., Bosch, D., Monié, P., Tardy, M., Maury, R.C., Hernández, J., Polvé, M., Yeghicheyan, D., Cotton, J., 1999. Late Jurassic oceanic crust and upper Cretaceous Caribbean plateau picritic basalts exposed in the Duarte igneous complex, Hispaniola. Journal of Geology, 107, 193-207.

Lapierre, H., Bosch, D., Dupuis, V., Polvé, M., Maury, R., Hernandez, J., Monié, P., Yeghicheyan, D., Jaillard, E., Tardy, M., de Lepinay, B., Mamberti, M., Desmet, A., Keller F., Senebier, F., 2000. Multiple plume events in the genesis of the peri-Caribbean Cretaceous oceanic plateau province. Journal of Geophysical Research, 105, 8403-8421.

Lázaro, C., García-Casco, A., Rojas Agramonte, Y., Kröner, A., Neubauer, F., Iturralde-Vinent, M., 2008. Fifty-five-million-year history of oceanic subduction and exhumation at the northern edge of the Caribbean plate (Sierra del Convento mélange, Cuba). Journal of Metamorphic Geology, 19-40. doi:10.1111/j.1525-1314.2008.00800.

Lebrón, M.C., Perfit, M.R., 1994. Petrochemistry and tectonic significance of Cretaceous island-arc-rocks, Cordillera Oriental, Dominican Republic. Tectonophysics, 229, 69-100.

Lewis, J.F., Amarante, A., Bloise, G., Jimenez, J.G., Dominguez, J., 1991. Lithology and stratigraphy of Upper Cretaceous rocks volcanic and volcaniclastic rocks of the Tireo Group, Dominican Republic and correlations with the Massif du Nord with Haiti. In: Mann, P., Draper, G., Lewis, J.F. (eds.). Geologic and tectonic development of the North America-Caribbean plate boundary in Hispaniola. Geological Society of America, 262 (Special Paper), 143-163.

Lewis, J.F., Escuder-Viruete, J., Hernaiz Huerta, P.P., Gutiérrez, G., Draper, G., 2002. Subdivisión Geoquímica del Arco Isla Circum-Caribeño, Cordillera Central Dominicana: Implicaciones para la formación, acreción y crecimiento cortical en un ambiente intraoceánico. Acta Geologica Hispanica, 37, 81-122.

Mann, P., 1999. Caribbean Sedimentary Basins: Classification and Tectonic Setting from Jurassic to Present. In: Mann, P. (ed.). Caribbean Basins. Sedimentary Basins of the World, 4, 3-31.

Martínez, F., Taylor, B., 2002. Mantle wedge control on backarc crustal accretion. Nature, 416, 417-420.

Mauffret, A., Leroy, S. 1997. Seismic stratigraphy and structure of the Caribbean igneous province. Tectonophysics, 283, l61-104.

Meschede, M., 1986. A method of discrimination between different types of mid-ocean basalts and continental tholeiites with the Nb-Zr-Y diagram. Chemical Geology, 56, 207-218.

Montgomery, H., Pessagno, E.A., Lewis, J.F., Schellekens, J., 1994. Paleogeography of Jurassic fragments in the Caribbean. Tectonics, 13, 725-732.

Montgomery, H., Pessagno, E.A., 1999. Cretaceous microfaunas of the Blue mountains, Jamaica, and of the Northern and Central Basement Complexes of Hispaniola. In: Mann, P. (ed.). Caribbean Basins. Sedimentary Basins of the World, 4, 237-246.

Nikolaeva, K., Gerya, T.V., Connolly, A.D., 2008. Numerical modelling of crustal growth in intraoceanic volcanic arcs. Physics of the Earth and Planetary Interiors, 171, 336-356.

Pearce, J.A., Peate, D.W., 1995. Tectonic implications of the composition of volcanic arc magmas. Earth and Planetary Science Annual Review, 23, 251-285.

Pearce, J.A., 2008. Geochemical fingerprinting of oceanic basalts with applications to ophiolite classification and the search for Archean oceanic crust. Lithos, 100, 14-48.

Pindell, J., Kennan, L., Maresch, W.V., Stanek, K.P., Draper, G., Higgs, R., 2005. Plate-kinematics and crustal dynamics of circum-Caribbean arc-continent interactions: Tectonic controls on basin development in Proto-Caribbean margins. In: Lallemant, A., Sisson, V.B. (eds.). Caribbean-South American plate interactions. Geological Society of America, 394 (Special Paper), 7-52.

Pindell, J., Kennan, L., 2009. Tectonic evolution of the Gulf of Mexico, Caribbean and northern South America in the mantle reference frame: an update. In. James, K., Lorente, M.A., Pindell, J. (eds.). The geology and evolution of the region between North and South America. Geological Society of London, 328 (Special Publications), 328, 1-55.

Pretorius, W., Weis, D., Williams, G., Hanano, D., Kieffer, B., Scoates, J.S., 2006. Complete trace elemental characterization of granitoid (USGSG-2,GSP-2) reference materials by high resolution inductively coupled plasma-mass spectrometry. Geostandards and Geoanalytical Research, 30(1), 39-54.

Révillon, S., Hallot, E., Arndt, N., Chauvel, C., Duncan, R.A., 2000. A Complex History for the Caribbean Plateau: Petrology, Geochemistry, and Geochronology of the Beata Ridge, South Hispaniola. Journal of Geology, 108, 641-661.

Salters, V.J.M., Stracke, A., 2004. Composition of the depleted mantle, Geochemistry, Geophysics, Geosystems, 5, Q05B07. doi: 10.1029/2003GC000597.

Sen, G., Hickey-Vargas, D.G., Waggoner, F., Maurasse, F., 1988, Geochemistry of basalts from the Dumisseau Formation. Southern Haiti: Implications for the origin of the Caribbean Sea crust. Earth Planetary Science Letters, 87, 423-437.

Shaw, D.M., 1970. Trace element fractionation during anatexis. Geochimica et Cosmochimica Acta, 34, 237-243.

Smith, G.P., Douglas, A., Karen, M.F., Leroy, M., Spahr, C.W., Hildebrand, J.A., 2001, A Complex Pattern of Mantle Flow in the Lau Backarc. Science, 292, 713-716.

Sinton, C.W., Duncan, R.A., Storey, M., Lewis, J., Estrada, J.J., 1998. An oceanic flood basalt province within the Caribbean plate. Earth Planetary Science Letters, 155, 221-235.

Sinton, C.W., Sigurdsson, H., Duncan, R.A., Leckie, R.M., Acton, G.D., Abrams, L.J., Bralower, T.J., Carey, S.N., Chaisson, W.P., Cotillon, P., Cunningham, A.D., Hondt, S.L., Droxler, A.W., Galbrun, B., Gonzalez, J., Haug, G.H., Kameo, K., King, J.W., Lind, I.L., Louvel, V., Lyons, T.W., Murray, R.W., Mutti, M., Myers, G., Pearce, R.B., Pearson, D.G., Peterson, L.C., Roehl, U., 2000. Geochronology and petrology of the igneous basement at the lower Nicaraguan Rise, Site 1001. Proceedings of the Ocean Drilling Program, Scientific Results, 165, 233-236.

Sun, S.S., McDonough, W.F., 1989. Chemical and isotopic systematics of oceanic basalts: Implications for mantle compositions and processes. In: Saunders, A.D., Norry, M.J. (eds.). Magmatism in the Ocean Basins. Geological Society of London, 42 (Special Publications), 313-345.

Talavera-Mendoza, O., Ruiz, J., Gehrels, G.E., Valencia, V.A., Centeno-García, E., 2007. Detrital zircon U/Pb geochronology of southern Guerrero and western Mixteca arc successions (southern Mexico): New insights for the tectonic evolution of southwestern North America during the late Mesozoic. Geological Society of America Bulletin, 119, 1052-1065. doi: 10.1130/B26016.1.

Taylor, B., Martínez, F., 2003. Back-arc basin systematics. Earth and Planetary Science Letters, 210, 481-497.

Thompson, P.M.E., Kempton, P.D., White, R.V., Saunders, A.D., Kerr, A.C., Tarney, J., Pringle, M.S., 2004. Elemental, Hf-Nd isotopic and geochronological constraints on an island arc sequence associated with the Cretaceous Caribbean Plateau: Bonaire, Dutch Antilles. Lithos, 74, 91-116.

Walker, J.A., Roggensack, K., Patino, L.C., Cameron, B.I., Otoniel, M., 2003. The water and trace element contents of melt inclusions across an active subduction zone. Contributions to Mineralogy and Petrology, 146, 62-77. doi:10.1007/s00410-003-0482-x.

Wallace, L.M., McCaffrey, R., Beavan, J., Ellis, S., 2005. Rapid microplate rotations and backarc rifting at the transition between collision and subduction. Geology, 33, 857-860.

Weis, D., Kieffer, B., Maerschalk, C., Barling, J., de Jong, J., Willians, G.A., Hanano, D., Pretorius, W., Scoates, J.S., Goolaerts, A., Friedman, R.M., Mahoney, J.B., 2006. High-precision isotopic characterization of USGS reference materials by TIMS and MC-ICP-MS. Geochemistry, Geophysics, Geosystems, 7, Q08006. doi: 10.1029/2006GC001283.

Winchester, J.A., Floyd, P.A., 1977. Geochemical discrimination of different magma series and their differentiation products using immobile elements. Chemical Geology, 20, 325-343.

Wood, D.A., 1980. The application of a Th-Hf-Ta diagram to problems of tectonomagmatic classification and to establishing the nature of crustal contamination of basaltic lavas of the British Tertiary volcanic province. Earth and Planetary Science Letters, 50, 11-30.

Manuscript received November 2010;
revision accepted June 2011;
published Online July 2011.

ELECTRONIC APPENDIX
Summary of analytical techniques

$^{40}Ar/^{39}Ar$ geochronology. Selected samples were crushed and sieved to obtain fragments ranging in the size range from 0.1 to 0.5mm. A hand magnet was passed over the samples to remove magnetic minerals and metallic crusher fragments/spall. The samples were rinsed in dilute nitric acid, washed in deionized water, rinsed and then air-dried at room temperature. Mineral separates were hand-picked, wrapped in aluminum foil and stacked in an irradiation capsule with similar-aged samples and neutron flux monitors (Fish Canyon Tuff sanidine, 28.02Ma; Renne et al., 1998). The samples were irradiated at the McMaster Nuclear Reactor in Hamilton, Ontario, for 56 MWH, with a neutron flux of $3x10^{16}$neutrons/cm^2. Analyses (n=54) of 18 neutron flux monitor positions produced errors of <0.5% in the J value. The mineral separates were step-heated at incrementally higher powers in the defocused beam of a 10W CO_2 laser (New Wave Research MIR10) until fused, at the Noble Gas Laboratory of the Pacific Centre for Isotopic and Geochemical Research, University of British Columbia. The gas evolved from each step was analyzed by a VG5400 mass spectrometer equipped with an ion-counting electron multiplier. All measurements were corrected for total system blank, mass spectrometer sensitivity, mass discrimination, radioactive decay during and subsequent to irradiation, as well as interfering Ar from atmospheric contamination and the irradiation of Ca, Cl and K. Isotope production ratios were ($^{40}Ar/^{39}Ar$)K=0.0302, ($^{37}Ar/^{39}Ar$)Ca =1416.4306, ($^{36}Ar/^{39}Ar$)Ca=0.3952, Ca/K=1.83($^{37}ArCa/^{39}ArK$). The plateau and correlation ages were calculated using Isoplot 3.09 software (Ludwig, 2003). Errors are quoted at the 2-σ (95% confidence) level and are propagated from all sources except mass spectrometer sensitivity and age of the flux monitor.

Whole rock geochemistry. Samples for geochemical analyses were obtained from the least weathered outcrops of the each unit. Sample locations are given as Universal Transverse Mercator in Table II. From a larger population, a subset of samples was screened in this study for the least alteration on the criteria of preservation of igneous textures, petrographic freshness, low values of loss on ignition (LOI), and coherent extended REE primitive mantle-normalized diagram for each given igneous suite. Selected samples were powdered in an agate mill, and analysed for major oxides and trace elements by inductively-coupled plasma-emission spectrometry (ICP-ES) and inductively-coupled plasma-mass spectrometry (ICP-MS) analysis with a $LiBO_2$ fusion, respectively. This analytical work was done at ACME Analytical Laboratories Ltd in Vancouver and results for selected samples of each geochemical group reported in Table II. For major elements oxides, the detection limits are less than 0.01% except for Fe_2O_3 (0.04%), P_2O_5 (0.001%) and Cr_2O_3 (0.002%). The detection limits for trace elements are typically less than 0.1ppm, except for Ba and Be (1ppm), Th (0.2ppm), Ga and Zr (0.5ppm); for some trace elements, they are as low as 0.05ppm. Analytical accuracy and reproducibility are estimated from measurements of duplicate analyses of samples, international rock standards CSC and STD O18 and blanks. The accuracy of the standards is within ± 10% of the suggested working values (Jenner et al., 1990), but generally better than ± 1% for refractory and rare earth elements. Duplicate analyses show reproducibility to be better than 1.0% except for the transition metals (e.g. Cr, Ni, Cu and Zn; <5.0%) and elements with very low concentrations (e.g. Tl), which show deviations of up to 10% (see below).

REFERENCES

Gerstenberger, H., Haase, G., 1997. A highly effective emitter substance for mass spectrometric Pb isotope ratio determinations. Chemical Geology, 136, 309-312.

Jenner, G.A., Longerich, H.P., Jackson, S.E., Fryer, B.J., 1990. A powerful tool for high-precision trace element analysis in earth sciences: evidence from analysis of selected U.S.G.S. reference samples. Chemical Geology, 83, 133-148.

Ludwig, K.R., 2003. User's manual for Isoplot 3.00 A Geochronological Toolkit for Microsoft Excel. Berkeley Geochronology Center, 4 (Special Publications), 71pp.

Renne, P.R., Swisher, C.C.III, Deino, A.L., Karner, D.B., Owens, T., DePaolo, D.J., 1998. Intercalibration of standards, absolute ages and uncertainties in $^{40}Ar/^{39}Ar$ dating. Chemical Geology, 145, 117-152.

Roddick, J.C., 1987, Generalized numerical error analysis with application to geochronology and thermodynamics. Geochimica et Cosmochimica Acta, 51, 2129-2135.

Weis, D., Kieffer, B., Maerschalk, C., Barling, J., de Jong, J., Willians, G.A., Hanano, D., Pretorius, W., Scoates, J.S., Goolaerts, A., Friedman, R.M., Mahoney, J.B., 2006. High-precision isotopic characterization of USGS reference materials by TIMS and MC-ICP-MS. Geochemistry, Geophysics, Geosystems, 7, 1-30. doi:10.1029/2006GC001283.

TABLE I | **Isotopic analyses of standards**

Sample #	$^{87}Sr/^{86}Sr$	Error (±2σ)	Cycles	$^{86}Sr/^{88}Sr$	$^{143}Nd/^{144}Nd$	Error (±2 σ)	Cycles	$^{145}Nd/^{144}Nd$	Error (±2 σ)	$^{146}Nd/^{144}Nd$
SRM987 600ng	0.710249	0.000008	123	0.1193						
SRM987 600ng	0.710249	0.000009	119	0.119						
SRM987 600ng	0.710250	0.000008	124	0.1194						
SRM987 600ng	0.710257	0.000009	125	0.1197						
SRM987 300ng	0.710256	0.000010	90	0.1190						
SRM987 600ng	0.710259	0.000007	124	0.1193						
La Jolla 150ng					0.511856	0.000006	114	0.348401	0.000004	0.7196
La Jolla 150ng					0.511854	0.000006	83	0.348402	0.000004	0.7204
La Jolla 150ng					0.511849	0.000006	116	0.348409	0.000004	0.7217
La Jolla 150ng					0.511857	0.000006	114	0.348399	0.000004	0.7203
La Jolla 150ng					0.511841	0.000007	116	0.348407	0.000004	0.7207
Average	0.710253	n=6			0.511851	n=5		0.348403		
Error	0.000009				0.000013			0.000008		

TABLE II | **Summary of ^{40}Ar-^{39}Ar incremental heating experiments of mineral separates**

5873I-SG9015	Whole-Rock Isotope		(sample/mineral)							
Laser Power(%)	Ratios 40Ar/39Ar	38Ar/39Ar	37Ar/39Ar	36Ar/39Ar	Ca/K	Cl/K	%40Ar atm	f 39Ar	40Ar*/39ArK	Age
2	59.563±0.018	0.319±0.047	0.841±0.026	0.291±0.054	8.124	0.057	101.97	0.3	- 1.155±4.619	- 21.63±87.07
2,2	22.037 0.007	0.076 0.057	0.816 0.015	0.084 0.036	8.59	0.01	91.99	1.89	1.685 0.902	31.11 16.52
2,4	10.992 0.006	0.034 0.033	0.692 0.016	0.034 0.031	7.332	0.003	72.12	4.34	2.948 0.314	54.08 5.67
2,6	8.533 0.007	0.025 0.040	0.488 0.017	0.022 0.038	5.158	0.001	54.81	5.81	3.716 0.243	67.91 4.36
2,8	8.084 0.007	0.022 0.057	0.460 0.016	0.019 0.032	4.866	0.001	51.09	6.66	3.819 0.180	69.75 3.23
3	7.224 0.007	0.020 0.059	0.443 0.015	0.017 0.029	4.721	0	48.51	6.63	3.577 0.150	65.42 2.69
3,3	6.404 0.005	0.017 0.053	0.467 0.013	0.011 0.021	5.009	0	39.14	15.99	3.814 0.071	69.66 1.27
3,5	5.770 0.005	0.019 0.046	0.427 0.015	0.010 0.022	4.577	0.001	34.08	12.44	3.696 0.066	67.56 1.18
3,7	5.515 0.005	0.021 0.045	0.573 0.013	0.009 0.034	6.158	0.001	31.06	13.29	3.699 0.094	67.60 1.69
4	5.876 0.005	0.027 0.039	0.754 0.016	0.011 0.034	8.115	0.002	32.74	10.2	3.831 0.109	69.97 1.96
4,5	8.189 0.005	0.047 0.028	1.636 0.013	0.017 0.025	17.713	0.007	38.3	9.23	4.952 0.125	89.95 2.22
6	11.990 0.005	0.087 0.020	3.407 0.013	0.025 0.021	37.208	0.016	42.66	13.22	6.873 0.159	123.66 2.76
Total/Average	7.825±0.001	0.033±0.006	5.968±0.001	0.014±0.006	10.967	0.008		100	4.177±0.024	
J=0.010323±0.000014			Volume 39ArK = 358.99							
Plateau Age = 68.40±0.75 Ma			(1s, including J-error of .5%)		MSWD = 0.63, probability = 0.71			71% of the 39Ar, steps 4 through 10		
Inverse isochron results: Model (±95%-conf.) on 7 points				Age = 67.8±4.8 Ma		40/36 intercept: 300±33, MSWD = 0.72, Probability = 0.61 (at J=.010323±.5% 1s)				

6JE13A	Hornblende		(sample/mineral)							
Power(%)	40Ar/39Ar	38Ar/39Ar	37Ar/39Ar	36Ar/39Ar	Ca/K	Cl/K	%40Ar atm	f 39Ar	40Ar*/39ArK	Age
2	40.880±0.015	0.088±0.026	0.718±0.020	0.143±0.021	7.898	0.011	97.57	3.27	0.959±0.906	17.78±16.71
2,3	12.379 0.019	0.035 0.036	0.674 0.023	0.035 0.026	7.673	0.003	75.75	10.63	2.954 0.275	54.19 4.97
2,6	13.673 0.015	0.041 0.028	0.544 0.020	0.036 0.026	6.139	0.005	69.35	8.96	4.130 0.291	75.33 5.20
2,9	11.852 0.016	0.028 0.054	0.447 0.020	0.029 0.037	4.979	0.002	61.86	7.3	4.440 0.334	80.85 5.95
3,2	7.296 0.018	0.025 0.044	0.194 0.024	0.012 0.036	2.126	0.002	37.47	12.35	4.476 0.156	81.50 2.78
3,5	6.299 0.018	0.017 0.037	0.191 0.023	0.008 0.038	2.128	0	28.96	17.28	4.398 0.123	80.11 2.19
3,8	6.154 0.012	0.022 0.050	0.307 0.021	0.008 0.060	3.462	0.001	27.88	17.61	4.364 0.149	79.50 2.66
4,1	5.648 0.009	0.021 0.045	0.198 0.018	0.006 0.050	2.184	0.001	22.4	13.37	4.288 0.104	78.14 1.86
5	5.913 0.012	0.023 0.046	0.184 0.027	0.008 0.043	1.972	0.002	24.02	9.22	4.371 0.115	79.62 2.05
Total/Average	9.016±0.003	0.026±0.007	2.019±0.002	0.017±0.006	3.7	0.003		100	4.098±0.036	
J = 0.010324±0.000014			Volume 39ArK = 314.28							
Plateau Age = 79.4±1.0 Ma			(1s, including J-error of .5%)		MSWD = 0.30, probability = 0.94			86.1% of the 39Ar, steps 3 through 9		
Inverse isochron results: Model (±95%-conf.) on 7 points				Age = 79.7±3.0 Ma		40/36 intercept: 293±18, MSWD = 0.35, Probability = 0.88, (at J=.010324±.5% 1s)				
Volumes are 1E-13 cm3 NPT			Neutron flux monitors: 28.02 Ma FCs (Renne et al., 1998)							
Isotope production ratios: (40Ar/39Ar)K=0.0302±0.00006, (37Ar/39Ar)Ca=1416.4±0.5, (36Ar/39Ar)Ca=0.3952±0.0004,								Ca/K=1.83±0.01(37ArCa/39ArK).		

Sample description

Sample 5873I-SG9015 is a basaltic flow from the Loma Los Guandules in the Restauración area. The basalt is composed of euhedral olivine phenocrysts (totally replaced by iddingsite and/or clay minerals), phenocrysts, and microcrysts of augite, plagioclase microlites, and opaque minerals. The mesostasia is devitrified glassy and vesicular.

Sample 6JE13A is a basaltic dike intruding the Constanza Formation of the Tireo group in the Constanza area. The textures are fine-grained intersectal to cryptocrystalline. It is composed of plagioclase, augitic clinopyroxene and hornblende micro-phenocrysts, and very-fine grained Fe-Ti oxides as accesory phases.

TABLE III | **Parameters used in forward melt models**

Modal abundances

	olivine	orthopyroxene	clinopyroxene	spinel	garnet
spinel lherzolite	0.5	0.3	0.15	0.05	0
garnet lherzolite	0.5	0.3	0.12	0	0.08

Partition coefficients -spinel lherzolite

Element	ol/liq	opx/liq	cpx/liq	sp/liq	Bulk D (sp)	P (sp)	Source	F=9%
La	0.0005	0.0031	0.03	0	0.0056	0.0188	0.234	2.6
Ce	0.0005	0.004	0.08	0.0005	0.0133	0.049	0.772	8.58
Sr	0.00004	0.0007	0.091	0	0.0137	0.0545	9.8	109
Nd	0.00042	0.012	0.088	0.0008	0.0168	0.0561	0.713	7.91
Zr	0.00131	0.021	0.18575	0.05	0.0371	0.1198	7.94	83.2
Sm	0.0011	0.02	0.299	0.0009	0.0508	0.1844	0.27	2.65
Eu	0.00805	0.053	0.3245	0.0009	0.0678	0.2098	0.107	0.94
Ti	0.015	0.086	0.35	0.1	0.0903	0.2406	798	6030
Gd	0.0011	0.065	0.35	0	0.0716	0.2282	0.395	3.39
Tb	0.0019	0.038	0.375	0.00075	0.0678	0.2351	0.075	0.66
Dy	0.0027	0.011	0.4	0.0015	0.0639	0.242	0.531	4.85
Ho	0.00785	0.028	0.41	0.00225	0.0731	0.2534	0.122	1.05
Er	0.013	0.045	0.42	0.003	0.0822	0.2647	0.371	2.99
Yb	0.02	0.08	0.45	0.0045	0.1006	0.2935	0.401	2.88

Partition coefficients -garnet lherzolite

Element	ol/liq	opx/liq	cpx/liq	gar/liq	Bulk D (gar)	P (gar)	Source	F=1.7%
La	0.0005	0.004	0.015	0.0007	0.0033	0.006	0.234	13.7
Ce	0.0005	0.004	0.038	0.017	0.0074	0.02	0.772	41.1
Sr	0.00004	0.0007	0.091	0.0007	0.011	0.0315	9.8	458
Nd	0.00042	0.012	0.0884	0.064	0.0198	0.0559	0.713	24.6
Zr	0.00076	0.018	0.1142	0.232	0.0394	0.1283	7.94	167
Sm	0.0011	0.02	0.1509	0.23	0.0443	0.1404	0.27	5.17
Eu	0.00805	0.053	0.14545	0.415	0.073	0.2133	0.107	1.34
Ti	0.015	0.086	0.14	0.6	0.1017	0.2863	798	7390
Gd	0.0011	0.065	0.16	1.2	0.1433	0.5117	0.395	2.68
Tb	0.0019	0.065	0.165	1.2	0.1443	0.5135	0.075	0.51
Dy	0.0027	0.065	0.17	2	0.215	0.8136	0.531	2.45
Ho	0.00785	0.065	0.175	2.5	0.2618	1.0024	0.122	0.47
Er	0.013	0.065	0.18	3	0.3085	1.1913	0.371	1.21
Yb	0.02	0.08	0.25	5.5	0.5427	2.1504	0.401	0.75

Partition coefficients are from Salters and Stracke (2004), 2.0 GPa for spinel lherzolite assemblage and 3.0 GPa for garnet lherzolite assemblage.
Values in italics are from Johnson et al. (1990). F=9% and F=1.7% are calculated melt compositions
for at the listed % of melting for spinel lherzolite and garnet lherzolite, respectively. P is the non-modal melt factor.